EFFECT OF ISOTOPIC COMPOSITION ON INFRARED ABSORPTION OF THIN FILMS OF LITHIUM FLUORIDE AND LITHIUM HYDRIDE

These for the Degree of Ph. D.
MICHIGAN STATE UNIVERSITY
Ramzi Hanna Misho
1961



This is to certify that the

thesis entitled

Effect of Isotopic Composition on Infrared Absorption of Thin Films of Lithium Fluoride and Lithium Hydride

presented by

Ramzi Hanna Misho

has been accepted towards fulfillment of the requirements for

PhD degree in Physics

D. J. Montgomery

Date November 16, 1961

O-169



ABSTRACT

EFFECT OF ISOTOPIC COMPOSITION ON INFRARED ABSORPTION OF THIN FILMS OF LITHIUM FLUORIDE AND LITHIUM HYDRIDE

by Ramzi Hanna Misho

The interaction of electromagnetic radiation with crystalline lattices is studied by observing the absorption of far-infrared radiation in thin films of certain simple substances evaporated on various substrates. To elucidate the nature of lattice vibrations, the isotopic composition of the absorbing substance is varied. The substances studied are lithium fluoride made from varying proportions of Li and Li in combination with F¹⁹, and lithium hydride made from varying proportions of Li and Li in combination with H and H. The substrates are polyethylene, potassium bromide, and cesium bromide. Observations are made in the wavelength region 10-40 microns, and at film temperatures of 300°K, 200°K, and 120°K. Each resulting spectrum is inspected for a principal absorption line and for subsidiary lines. The shape of the principal line is examined, and the variation of the parameters characterizing it, are studied with respect to isotopic composition, temperature, and nature of the substrate.

So far as dependence on isotopic mass is concerned, the position of maximum absorption for isotopically-pure LiF and LiH follows quantitatively the predictions of the elementary portion of the Born theory, namely, that the dispersion wavelength is proportional to the square root of the reduced mass. The positions of the absorption maxima for isotopically-impure LiF 19 are intermediate between those for pure Li F and Li F, and are in agreement with the elementary Born theory if the average isotopic masses are used. The positions of the absorption maxima for isotopically-impure LiH do not follow any simple law. So far as dependence on temperature is concerned, the dispersion wavelengths for pure and impure LiF and LiH--with the exception of Li H and Li⁷H¹--decrease slightly with decreasing temperature, as would be expected theoretically. The absorption bands of all the pure and impure LiF and LiH become deeper and narrower with decreasing temperature, in qualitative agreement with theory. The effect of substrate, though not pronounced, is complicated and difficult to understand. We may conclude generally that although the main features of the interaction of electromagnetic radiation with crystalline lattices are understood, most of the details cannot be predicted quantitatively, and great improvement in the theory is needed.

ABSORPTION OF THIN FILMS OF LITHIUM FLUORIDE AND LITHIUM HYDRIDE

Ву

RAMZI HANNA MISHO

A THESIS

Submitted to
Michigan State University
in partial fulfillment of the requirements
for the degree of

DOCTOR OF PHILOSOPHY

Department of Physics and Astronomy

G 2020% 5/24/62

ACKNOWLEDGMENTS

I would like to express my deep appreciation to Professor D. J. Montgomery for suggesting the problem investigated in this thesis and for his constant counsel and guidance during the four years I spent on the campus of Michigan State University. His insight, broad perspective, understanding, and patience have always been a source of encouragement.

My sincere appreciation and thanks go to:

- Mr. Kwok Fai Yeung who did most of the calculations and helped in the experimental work;
- Mr. Charles Kingston and his technical staff for building the lowtemperature cells and rebuilding the evaporator;
- Dr. Harry Eick of the Department of Chemistry for the use of a dry box and other equipment;
- Miss Suzan Langham for weighing and mixing the various compositions used in the experiment.

Major financial support for this work was provided by the U.S.

Air Force Office of Scientific Research. The project was initiated with the help of an All-University Research Grant from Michigan State University and was continued through support from the U.S.

Atomic Energy Commission. This help is gratefully acknowledged.

TABLE OF CONTENTS

Chapter			Page
I.	INTRODUCTION		
		Statement of Problem	8
II.	THE	CORETICAL OBSERVATIONS	10
III.	EXF	PERIMENTAL TECHNIQUE	23
	A.	Apparatus	23
	B.	Film Preparation	29
	c.	Temperature Measurement	35
IV.	EXPERIMENTAL RESULTS		
	A.	Lithium Fluoride	37
	в.	Lithium Hydride	63
v.	DISCUSSION OF EXPERIMENTAL RESULTS		
	A.	Dispersion Wavelength $\lambda_0 = 2\pi c/\omega_0$	81
	в.	Damping Constant γ/ω_0	85
REFERI	ENCE	S CITED	93

LIST OF TABLES

Table		Page
1.	Compositions of LiF^{19} and their reduced masses	52
2.	Value of γ/ω_0 for the various ${\rm LiF}^{19}$ compositions	62
3.	Compositions of LiH, their average reduced masses and their dispersion wavelengths	69
4.	Effect of isotopic mass on infrared dispersion wavelength	82
5.	Effect of isotopic composition on dispersion wave-	84

LIST OF FIGURES

Figure		Page
1.	Schematic version of infrared spectrum for a thin absorbing film	16
2.	General view of apparatus	25
3.	Cut-away view of the low-temperature sample holder	26
4.	Detailed sectional view of the sample holder	27
5.	Stray-radiation run	38
6.	Atmospheric-absorption run	39
7-17.	Infrared absorption spectra of thin films of LiF ¹⁹ containing varying proportions of Li ⁶ F ¹⁹ and Li ⁷ F ¹⁹ as indicated on individual figures. Temperature, 300° K; substrate, polyethylene sheet	40-50
18-19.	Infrared absorption spectra of thin films of LiF ¹⁹ containing 30% Li ⁶ F - 70% Li ⁷ F (Figure 18) and 70% Li ⁶ F - 30% Li ⁷ F (Figure 19). Temperatures, 300°K and 200°K; substrate, polyethylene	53-54
20-21.	Infrared absorption spectra of thin films of LiF ¹⁹ containing 30% Li ⁶ F - 70% Li ⁷ F (Figure 20) and 70% Li ⁶ F - 30% Li ⁷ F (Figure 21). Temperatures, 300°K and 120°K; substrate, polyethylene	55-56
22.	Infrared dispersion wavelength for LiF ¹⁹ films evaporated onto sesium-bromide substrate, as a function of isotopic composition x. Temperature: 300° K and 120°K	58
23.	Infrared dispersion wavelength for LiF ¹⁹ films evaporated onto polyethylene substrate, as a function of isotopic composition x. Temperatures: 300°K, 200°K, and 120°K	59
24.	Separation of main absorption peak from minor ones, for spectrum of Li ⁶ F ¹⁹ film deposited onto polyethylene substrate. Temperature: 200°K	61

25.	Lines of equal reduced mass for lithium hydride made of varying proportions of Li ⁶ , Li ⁷ and H ¹ , H ²	64
26.	Infrared absorption spectrum of Li ⁷ l film evaporated onto KBr substrate. Temperatures: 300°K, 120°K	66
27.	Infrared absorption spectrum of Li ⁷ H film evaporated onto KBr substrate. Temperatures: 300°K, 120°K	67
28.	Infrared absorption spectrum of Li ⁷ H ¹ film, on which is superimposed the spectrum of Li ⁷ H ² with abscissa multiplied by square root of reduced masses. Substrate: KBr; temperature, 300°K	68
29.	Infrared absorption spectrum of Li ⁷ H ¹ film on which is superimposed the spectrum of Li ⁷ H ² with abscissa multiplied by square root of reduced masses. Substrate: KBr; temperature, 120°K	71
30.	Infrared absorption spectrum of Li ⁷ l evaporated onto KBr substrate. Temperatures: 125°K, 177°K, 234°K, and 318°K	72
31.	Infrared absorption spectra of Li ⁷ H ¹ evaporated onto KBr substrate. Temperatures: 310°K, 357°K, 400°K, and 440°K	73
32.	Infrared absorption spectrum of Li ⁶ H film evaporated onto polyethylene substrate, after reaction with atmosphere. Temperatures: 300°K, 120°K	75
33.	Infrared absorption spectrum of Li ⁷ H film evaporated onto polyethylene substrate, after reaction with atmosphere. Temperatures: 300°K, 120°K	76
34.	Plot of $(\lambda_+\lambda)^{1/2}$ as a function of transmission T for a spectrum of $\text{Li}^7 \text{H}^1$ evaporated onto KBr substrate. Temperature: 120°K	7 8
35.	Separation of main absorption peak from minor ones, for spectrum of Li ⁷ H ¹ film deposited on KBr substrate. Temperature: 120°K	79
36.	Plot of $(\frac{\lambda}{\lambda_0} - \frac{\lambda_0}{\lambda})^2$ as a function of $\frac{1}{T-T} - \frac{1}{T-T}$ for a spectrum of Li ⁷ H ¹ evaporated onto KBr substrate.	
	Temperature: 120° K	80

37.	Dependence of infrared dispersion wavelength on absolute temperature for LiF ¹⁹ films of various		
	isotopic compositions evaporated onto CsBr and onto polyethylene	86	
38.	Dependence of infrared dispersion wavelength on absolute temperature for LiH and LiD films eva-	87	
	porated onto KBr	01	
39.	Plot of γ/ω_0 against isotopic compositions for LiF evaporated onto polyethylene and recorded at $300^{\rm o} K \dots$	90	
40.	Variation of γ with absolute temperature for Li ⁷ F ¹⁹	91	

I. INTRODUCTION

This thesis deals with the interaction of electromagnetic radiation with the solid crystalline phase. Every substance has its own characteristic spectrum, possessing selective absorption at certain frequencies in the spectrum. The spectral characteristics are determined by the atomic masses, the configuration in space, and the binding forces present. Around 1950, relatively large amounts of stable isotopes became available, and it became possible to utilize these substances in the study of bulk properties of matter. By use of isotopes of the same element, the atomic mass can be changed while the atomic force field is kept the same. The dependence of physical properties on the mass is usually simple, whereas the dependence of force field is very complicated. Hence, one may sometimes make comparisons between isotopes of the same element when it is not practical between different elements. The characteristic energy of the far infrared radiation matches that of the lattice vibrations, and therefore depends in the first order on isotopic mass. A program using the isotopic mass as a probe for the study of the physical properties of matter was started a few years ago in our laboratory. The work described in this paper constitutes an extension and refinement of this program. Besides using the isotopic mass as the only variable under consideration, one may also use the

isotopic composition as another variable. A new type of phenomenon may be expected to appear if one uses a mixture of various proportions of the stable isotopes. Specific heat, electrical resistivity, infrared absorption spectrum and other phenomena depending on lattice vibration spectrum may all be expected to show modified behavior.

In the experiments discussed in this paper, the isotopic mass is used as a probe to study the infrared absorption spectra of ionic and partially ionic crystals. The spectrophotometers available to us cover the region of the spectrum from 2 to nearly 40 microns. To get the frequency of vibrations high enough to bring the infrared absorption bands for lattice vibrations into accessible wave lengths, one has to use elements as light as possible, with binding forces as strong as possible. The alkali halides are excellent materials for study, because of their simple structure and high electric moment. One chooses lithium because it is light and because its isotopes Li and Li are readily obtainable and give large relative mass difference. The lightest halogen is fluorine; it has only one stable isotope, F¹⁹. Lithium fluoride, LiF, is a well known substance, and is easy to handle; but its characteristic absorption bands are beyond 30 microns, an inconvenient region of the spectrum. One then expects easy preparation and handling, but difficult observation.

Lithium fluoride, like the other alkali halides, possesses ionic crystal structure. The optical properties of many of these alkali

halides have been studied previously. These properties are governed, in the infrared region of the spectrum, primarily by the vibrations of the crystal lattice. In the literature the experimental results are compared with theories of lattice vibrations, and in many cases an explanation that is more or less plausible can be given. In an ionic crystal, ions may be assumed as being charged mass points interconnected by approximately harmonic forces. The fundamental optical mode of vibration of such a system has a simple dependence on the masses of the constituent ions. Besides the fundamental optical mode, the other secondary modes may exist which cannot be explained on the simple model described above. Several suggestions have been given in attempted explanation of the existence of these secondary modes. Lax and Burstein (1) suggested a possible deformation of the electron cloud about the atoms during lattice vibrations, leading to a second-order electric moment, and in turn to the appearance of auxiliary bands in the infrared absorption and reflection spectra of the ionic crystals. Barnes, Brattain, and Seitz (2) suggested that the secondary structure is due to the anharmonicity in the lattice vibrations. Szigeti (3) has combined both effects in a systematic general treatment of this model. Wallis and Maradudin (4) in a paper discussing the impurity-induced infrared absorption suggested that the presence of isotopic impurities in the crystal lattice leads to a

broad absorption on the low-frequency side of the main maximum even when the harmonic approximation is made.

Barnes (5) was the first to study experimentally the far-infrared absorption spectrum of natural LiF. He found that the absorption maximum is at a wave length of 32.6 ± 0.3 microns, with one side band in the 25 to 28 microns region and another in the 18 to 20 microns region. Stevenson and Nettley (6) studied the infrared transmission limits and reflectivity of Li⁶F¹⁹ and Li⁷F¹⁹, and found that the reflection measurements give peaks at 16.7 microns for Li F , and at 15.8 microns for Li⁷F¹⁹. The ratio of these wave lengths agrees with the simple theory. Other work has also been carried on by various investigators on the optical properties of natural and isotopically-enriched lithium fluoride at various temperatures and under different circumstances. For example, Heilman (7) measured the optical constants n and k for LiF in the region of the infrared reststrahlen band. Hohls (8) studied the dispersion and the absorption of LiF in the infrared. Klier (9) studied the temperature dependence of the optical constants of LiF in the infrared. Hass and Ketelaar (10) measured the width of the infrared reflection bands of LiF and gave values for its dielectric constant, normal index of refraction, and dispersion wave length. Gottleib (11) studied the optical properties of crystals of natural LiF, and of Li F and Li F at various temperatures. Montgomery and Misho reported

briefly some results on the dispersion wave length for isotopicallymixed lithium fluoride.

As mentioned earlier in this chapter, the characteristic absorption of lithium fluoride lies beyond 30 microns, a region where experiment is difficult. To bring the region of characteristic absorptions to more convenient wave lengths, one must either decrease the mass of the ions, or increase the binding force. One should restrict his choice to monovalent elements in order to keep simple structures. The Group-I elements have in their outer shell a single s-electron that can be easily removed. The Group-VII elements have two s-electrons and five p-electrons that can easily take on an additional electron to form a closed shell. From this point of view, hydrogen may be considered to be either the lightest alkali metal or the lightest halogen, since its single s-electron may either be removed, or may take on another electron to form a closed shell consisting of a pair of ls-electrons. Thus we are led to consider the use of hydrogen fluoride or of lithium hydride as light "alkali halides."

Hydrogen fluoride does not crystallize as an ionic crystal but instead as a molecular crystal. Infrared spectroscopy will then yield information only about its intramolecular vibrations, rather than its lattice vibrations, the topic of interest in the present work. Therefore, we are left with lithium hydride, which forms a partially-

ionic sodium-chloride structure. The isotopic proportions of both cation and anion can be varied. We use only Li and Li, and H and H. But one could also use H, despite its radioactivity, if there were really need for it. For the lightest lithium hydride (Li H), the characteristic absorption band is around 17 microns, a region quite easy to work in. For the heaviest (nonradioactive) lithium hydride (Li⁷H²), the characteristic absorption is around 22.5 microns, a region still much easier to work with than the 30micron region characteristic of lithium fluoride. Therefore, use of the hydride gave us the great advantage of working in a much more accessible region of the spectrum. On the other hand, the use of the hydride presents several liabilities: theoretically, the hydride is not ionic; it seems to have high deformability of the charge clouds; its chemical behavior is in general more complicated than that of the true alkali halides; it is extremely reactive with water vapor; and thus in thin-film form, can react with the least amount of water vapor (and perhaps other substances) to produce a strong chemical transformation resulting in profound changes in the spectrum. Spectral bands due to the contamination by lithium hydroxide are then separated with difficulty from possible side bands occurring in the pure substance alone. It is possible, however, by appropriate evaporating techniques and by variation of temperature to identify the various bands.

The visible spectrum of gaseous lithium hydride was studied as early as 1925 (13) by Watson. The absorption and band spectra of gaseous Li H were studied by Nakamura (14) in 1929, and its molecular constants were calculated. The first work on the isotopic shift of the band spectra of LiH and LiD was reported by F. H. Crawford and T. Jorgensen (15) in 1934. The infrared spectrum of gaseous LiH was studied by Klemperer (16) in 1955, and the near-ultraviolet absorption spectrum of LiH and LiD was studied by Velasco (17) in 1957. Filler and Burstein (18) studied the infrared lattice vibration spectrum of natural lithium hydride. Their reflection spectra from single crystals in the range 2-50 microns showed strong peak in the region from 9 to about 18 microns with a minimum around 8 microns. The first infrared absorption spectrum of solid lithium hydride was obtained by Zimmerman (19), who worked with solid thin films of isotopically-pure LiH and LiD at room temperature. The characteristic absorption wave lengths were in agreement with the simple theory. Zimmerman also determined the infrared absorption spectra of thin films of Li H made up of different isotopic compositions with respect to hydrogen. No simple theoretical interpretation was possible.

Besides LiF and LiH, there are of course other substances that could be used. Studies on compounds composing Group-II elements

in combination with Group-VI elements appear promising; Mg O and Mg O, for example, is a useful case. One of course can also get O^{16} , O^{17} and O^{18} , but their rare isotopes are much too expensive in high purity. Other combinations of groups that would be of interest are Group-III, Group-V compounds. Here the isotopic proportion of the B in combination with the anions N, p and perhaps As could be varied. Elemental semi-conductors of Group-IV - Si, Ge, and perhaps C and Sn - could be studied also. However, sample preparation would be more complicated and observations more difficult. Certain ternary compounds, for example, LiBH4, CaCO3, and certain other elements - for example, S or Se - and some organic compounds could also be considered. The study of crystalline acids and amides, where hydrogen bands are of great importance in determining the crystal structure, would be of particular interest. Moreover, certain hydrides of more complicated structures, for example, decaborane, $B_{10}M_{14}$ would seem to constitute extremely interesting subjects for further study.

Statement of Problem

The infrared absorption spectra of thin films of Li⁶F¹⁹ and Li⁷F¹⁹, and of films made up of different isotopic compositions of the Li⁶F¹⁹ and Li⁷F¹⁹, and evaporated on two different substrates (polyethylene and cesium bromide), are obtained at three different

temperatures (approximately 300°K, 200°K, 120°K). The infrared absorption of Li⁶H¹, Li⁶H², Li⁷H¹ and Li⁷H², and of films made up of different isotopic compositions of Li⁶H¹ and Li⁶H² and of Li⁷H¹ and Li⁷H², and evaporated on three different substances (polyethylene, potassium bromide and cesium bromide), are obtained at two different temperatures (approximately 300°K and 120°K).

The measurements at low temperatures are made with the hope of identifying certain bands which may be due to contamination, or which may represent genuine side bands occurring in the original compounds. The resulting spectra are analyzed to see how isotopic mass affects the presence, shape, and position of absorption bands, and to see what light can be shed on the general mechanism of interaction of electromagnetic radiation with lattice vibrations.

II. THEORETICAL OBSERVATIONS

In this chapter, the derivation of the dispersion formula for a simple ionic crystal is reviewed, the transmission coefficient for a thin film is quoted, and a few of the theoretical results derived in Born and Huang (20) are analyzed and rewritten in a form suitable for the experimental results to be discussed subsequently.

To derive the dispersion formula for an ionic crystal, we assume that the macroscopic theory is fully contained in the following pair of phenomenological equations:

$$\frac{\ddot{\mathbf{W}}}{\ddot{\mathbf{W}}} = (\frac{\epsilon_{0} - \epsilon_{\infty}}{4\pi}) \qquad \omega_{0} \mathbf{E} - \omega_{0}^{2} \mathbf{W} - \gamma \mathbf{W}$$

$$\underline{\mathbf{P}} = \left(\frac{\epsilon_{\infty} - 1}{4\pi}\right) \underline{\mathbf{E}} + \left(\frac{\epsilon_{\infty} - \epsilon_{\infty}}{4\pi}\right)^{\frac{1}{2}} \omega_{\infty} \underline{\mathbf{W}}.$$

Here <u>W</u> is the displacement of a positive ion relative to a negative one, multiplied by the square root of the reduced mass per unit volume;

P, and E are the dielectric polarization and electric field as defined in Maxwell's equations;

- ϵ_0 is the low-frequency dielectric constant;
- ϵ_{∞} is the high-frequency dielectric constant;
- ω is the circular infrared dispersion frequency.

To get the dispersion formula, one substitutes the following periodic solutions into the above equations:

We get:

et:
$$-\omega^{2}\underline{W} = \left(\frac{\epsilon_{o} - \epsilon_{\infty}}{4\pi}\right)^{2} \omega_{o}E - (\omega_{o}^{2} + i\omega\gamma) W$$

$$\underline{\mathbf{P}} = (\frac{\epsilon_{\infty} - 1}{4\pi})\underline{\mathbf{E}} + (\frac{\epsilon_{0} - \epsilon_{\infty}}{4\pi})^{\frac{1}{2}} \quad \omega_{0}\underline{\mathbf{W}}$$

Eliminating W from these two equations,

$$\underline{P} = \left[\frac{(\epsilon_{\infty} - 1)}{4\pi} + \frac{(\epsilon_{0} - \epsilon_{0}) \omega_{0}^{2}}{4\pi (\omega_{0}^{2} - \omega^{2} - i\omega_{Y})} \right] \underline{E},$$

and comparing this result with Maxwell's equation,

$$\underline{\mathbf{D}} = \underline{\mathbf{E}} + 4\pi \, \underline{\mathbf{P}} = \epsilon \underline{\mathbf{E}} ,$$

we obtain the dispersion formula:

$$\epsilon = \epsilon_{\infty} + \frac{\left(\epsilon_{0} - \epsilon_{\infty}\right)}{2} \qquad (1)$$

$$1 - \left(\frac{\omega}{\omega}\right) - i\left(\frac{\omega}{\omega}\right)\left(\frac{\gamma}{\omega}\right)$$

In the experiment described in the following chapters, the transmission of the infrared light through thin films of LiF and LiH is studied. An expression for the transmission of light of a given frequency ω incident normally on a plate of thickness d is given by:

$$T = \frac{1}{1 + i\omega (\frac{d}{2c}) (\bar{n}^*^2 - \bar{n}^2)}$$
 (2)

where n is equal to ϵ , the complex dielectric constant.

From this expression one may show easily that for very thin films suspended in air, the minimum transmission occurs exactly at the dispersion frequency. The films studied in the experiment described in this paper are actually deposited on thick substrates. The reflectivity at the film-substrate surface is given by $[(n-n_1)/(n+n_1)]^2$, where n is the refractive index of the substrate and n_1 that of the film. A further loss by reflection occurs at the substrate-air boundary, where the reflectivity ρ is $[(n-1)/(n+1)]^2$. The loss in transmitted intensity through reflection is approximately the sum of the losses at the two interfaces. For example the refractive index of LiF in the infrared is about 1.4, for CsBr about 1.6; here the losses by reflection amount to about 6%. refractive index of LiH is about 1.6, that of KBr is about 1.5; if KBr is used as substrate for LiH film, about 4% of light intensity is lost.

From equation (1) one can write:

$$\epsilon^* = \epsilon_{\infty} + \frac{(\epsilon_{o} - \epsilon_{\infty})}{1 - (\frac{\omega}{\omega_{o}})^2 + i(\frac{\omega}{\omega_{o}})(\frac{\gamma}{\omega_{o}})}$$

and

$$\epsilon^* - \epsilon = (\epsilon_0 - \epsilon_{\infty}) \frac{-2i \left(\frac{\omega}{\omega_0}\right) \left(\frac{\gamma}{\omega_0}\right)}{\left[1 - \left(\frac{\omega}{\omega_0}\right)^2\right]^2 + \left(\frac{\omega}{\omega_0}\right)^2 \left(\frac{\gamma}{\omega_0}\right)^2}$$

The expression for T can now be written as

$$T = \frac{\left[1 - \left(\frac{\omega}{\omega}\right)^{2}\right]^{2} + \left(\frac{\omega}{\omega}\right)^{2} \left(\frac{\gamma}{\omega}\right)^{2}}{\left[1 - \left(\frac{\omega}{\omega}\right)^{2}\right]^{2} + \left(\frac{\omega}{\omega}\right)^{2} \left(\frac{\gamma}{\omega}\right)^{2} + \frac{\omega d}{c} \left(\frac{\omega}{\omega}\right) \left(\frac{\gamma}{\omega}\right) \left(\epsilon_{o} - \epsilon_{\infty}\right)} \qquad (3)$$

We now make the following substitutions:

$$x = \left(\frac{\omega}{\omega}\right)^2 = \left(\frac{\lambda}{\lambda}\right)^2$$

$$a = \left(\frac{\gamma}{\omega}\right)^2$$

$$\frac{1}{\hat{a}} = (\frac{d}{c}) (\epsilon_0 - \epsilon_\infty)$$

$$\frac{Y}{3} = \beta$$

Then T =
$$\frac{(1-x)^2 + ax}{(1-x)^2 + ax + \beta x}$$
 = $\frac{\frac{1}{x} + x - (2-a)}{\frac{1}{x} + x - (2-a-\beta)}$

We make the further substitutions:

$$y = \frac{1}{x} + x$$

$$A = 2 - a$$

$$B = \beta$$

and
$$1 - C = T$$
.

Then: 1 - C =
$$\frac{(y-A)}{y-(A-B)}$$

or:
$$y = \frac{B}{C} + (B - A)$$
(4)

Equation (4) represents a straight line when y is plotted against $\frac{1}{C}$, with slope

$$m = B = (\frac{\gamma d}{c})(\epsilon_0 - \epsilon_0)$$

and intercept

$$b = B - A = (\frac{\gamma d}{c})(\epsilon_0 - \epsilon_\infty) - 2 + (\frac{\gamma}{\omega_0})^2$$
.

From these equations one can solve for the damping constant γ :

$$\gamma = \omega \sqrt{b - m + 2} \qquad (5)$$

where ω_0 is determined from inspection of the absorption spectrum. Then b and m can be read directly from the plot of y vs. $\frac{1}{C}$.

Rewriting equation 4, we find

$$\frac{1}{T} = \frac{(1-x)^2 + ax + \beta x}{(1-x)^2 + ax}$$

$$= 1 + \frac{\beta}{(\frac{1}{x} + x - 2 + a)}$$

$$= 1 + \frac{\left(\frac{\gamma d}{c}\right) \left(\epsilon_{o} - \epsilon_{\infty}\right)}{\left(\frac{\omega}{\omega_{o}} - \frac{\omega}{\omega}\right)^{2} + \left(\frac{\gamma}{\omega_{o}}\right)^{2}}$$

$$= 1 + \frac{\left(\frac{\gamma d}{c}\right) \left(\epsilon_{o} - \epsilon_{\infty}\right)}{\left(\frac{\lambda}{\lambda} - \frac{\lambda}{\omega}\right)^{2} + \left(\frac{\gamma \lambda}{2\pi c}\right)^{2}}$$

For maximum $\frac{1}{T}$, T equals T_{minimum} , and minimum transmission occurs at $\lambda = \lambda_0$. Moreover, as denoted in Figure 1, a schematic illustration of the course of the absorption, there are two wavelengths λ_+ and λ_- for which the transmission has a given value $T > T_{\text{min}}$. For each pair

$$\lambda_{+}\lambda_{-} = \lambda_{0}^{2} \qquad (6)$$

Equation 6 shows the symmetry of the absorption spectrum around $\lambda_0, \ a \ \text{fact which is of much help in the separation of the superimposed peaks.}$

We once more rewrite equation (4) in the following form:

$$\frac{1}{T} = 1 + \frac{\beta}{M + a}$$

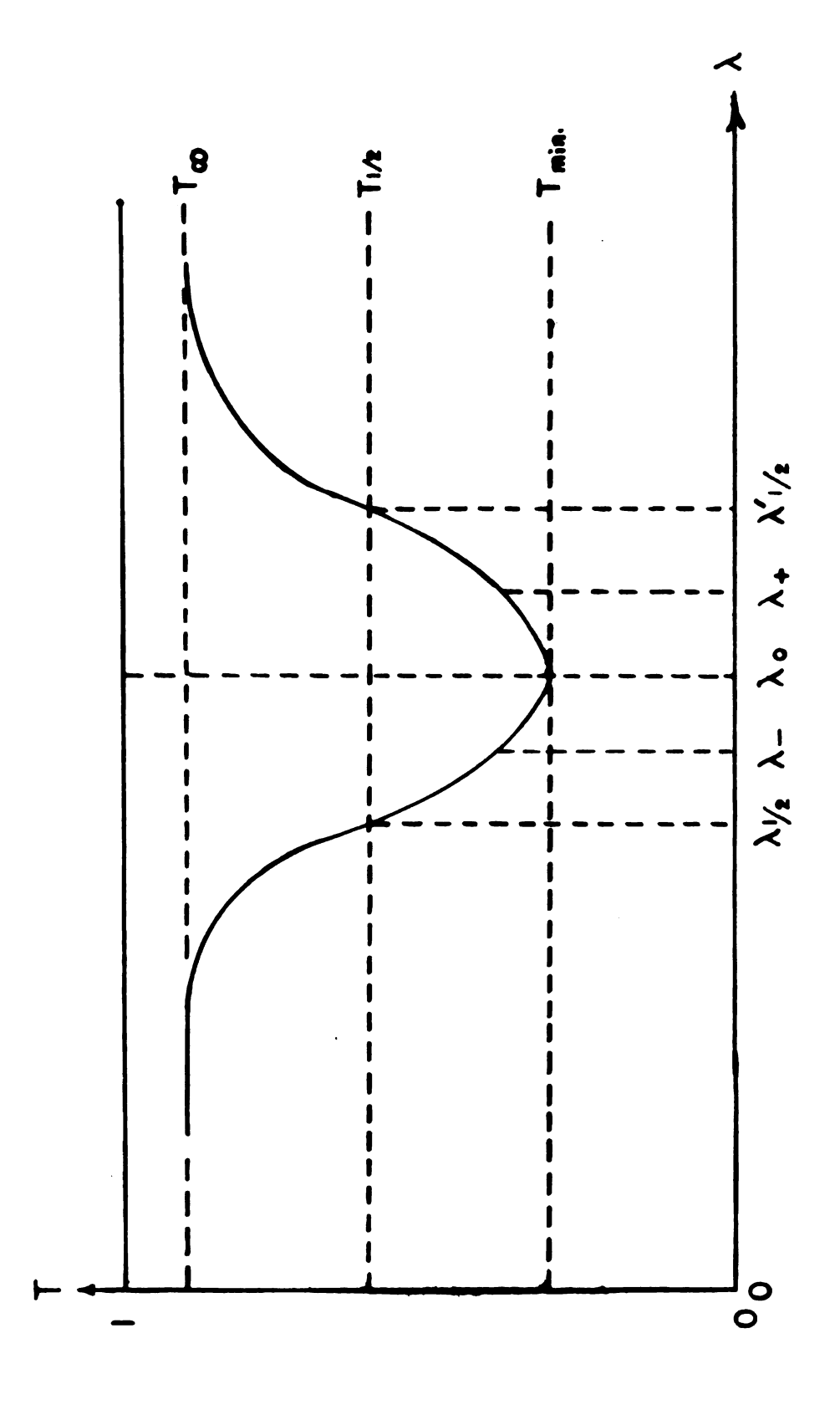
where

$$M = \left(\frac{\omega}{\omega} - \frac{\omega}{\omega}\right)^2.$$

It is necessary to replace $\frac{1}{T}$ by $\frac{T_{\infty}}{T}$ where T_{∞} is defined as shown in figure 1, since there is other absorption besides the main one (for an ideal case, where only the main absorption peak is present, $T_{\infty} = 1$).

$$\frac{T}{T} = \frac{[M+a+\beta]}{M+a}$$

and



Schematic version of infrared spectrum for a thin absorbing film. Here the transmission T is plotted against wavelength λ_{o} . Minimum transmission occurs at the dispersion wavelength λ_{o} . The

meaning of the other symbols is given in the text.

FIGURE 1

$$\frac{T_{\infty}}{T_{\min}} = \frac{a + \beta}{a}$$

$$M = -(\alpha + \beta) + \frac{T_{\infty}\beta}{T_{\infty} - T}$$

$$= T_{\infty} \beta \left(\frac{1}{T_{\infty} - T}\right) - (\alpha + \beta) \qquad (7)$$

Equation (7) represents a straight line plotted in the M, $\frac{1}{(T_{\infty}-T)}$ plane with a slope $T_{\infty}\beta$ and an intercept $(a+\beta)$. Here T_{∞} can be found directly from the spectrum. $T_{\infty}\beta$ and $(a+\beta)$ can be read directly from the plot of equation (7).

The thickness d of the film can now be calculated, since

$$\beta = (\frac{\gamma d}{c}) (\epsilon_0 - \epsilon_0)$$
 and $\gamma = \omega_0 \sqrt{a}$.

Therefore

$$d = \frac{c\beta}{\gamma(\epsilon_0 - \epsilon_0)} = \frac{\beta\lambda_0}{2\pi \sqrt{a}(\epsilon_0 - \epsilon_0)}$$

Of course this procedure provides in addition a means for calculating the damping constant γ .

It is possible also to derive expressions for a and β , and thus for γ and d, using $T_{1/2}$ and $M_{1/2}$ as defined in figure 1, corresponding to $\lambda_{1/2}$

$$T_{1/2} = (1/2) (T_{\infty} + T_{\min}),$$

or

$$\frac{T_{1/2}}{T_{\infty}} = \frac{1}{2} \left(1 + \frac{a}{a+\beta}\right)$$

also

$$\frac{T_{1/2}}{T_{\infty}} = \frac{M_{1/2} + \alpha + \beta}{M_{1/2} + \alpha}.$$

Therefore

$$M_{1/2} = \alpha + \beta = \left(\frac{\lambda_{1/2}}{\lambda_0} - \frac{\lambda_0}{\lambda_{1/2}}\right)^2$$
,

and

$$\frac{T_{\min}}{T_{\infty}} = \frac{M_{1/2} - \beta}{M_{1/2}},$$

from which

$$\beta = M_{1/2} \left(1 - \frac{T_{\min}}{T_{\infty}}\right),$$

and

$$\alpha = M_{1/2} - \beta = M_{1/2} (\frac{T_{\min}}{T_{\infty}}),$$

so that

$$d = \frac{c \beta}{\omega_0 \sqrt{\alpha} \left(\epsilon_0 - \epsilon_0\right)}$$

$$= \frac{\lambda_{o} M_{1/2} (1-T_{min}/T_{\infty})}{2\pi \sqrt{M_{1/2} \frac{T_{min}}{T_{\infty}} (\epsilon_{o} - \epsilon_{\infty})}}$$

or

and

$$\gamma = \frac{2\pi c}{\lambda_o} \left(\frac{\lambda_{1/2}}{\lambda_o} - \frac{\lambda_o}{\lambda_{1/2}} \right) \sqrt{\frac{T_{\min}}{T_{\infty}}} \qquad (9)$$

Here the quantities λ_0 , $\lambda_{1/2}$, λ_0 and λ_0 are given in the literature.

The preceding analysis provides a method for the measurement of the damping constant γ and the film thickness d. In principle, it provides a method for separation of the main absorption peak from the minor side peaks.

To get reasonable results, it is desirable that the spectrum be clean, and free from extraneous atmospheric absorption bands. Now all the spectra of lithium fluoride are recorded in the region 15 to 40 microns. The region from 24 to 40 microns is full of water absorption bands that interfere with the LiF spectrum and introduce inaccuracy in the true position of the minimum absorption. On the other hand, the spectra of lithium hydride are recorded in the region 10 to 28 microns. This region is relatively free of atmospheric absorption, but there is much trouble from spurious peaks due to lithium hydroxide and other compounds contaminating the film itself. Nevertheless, the above method of analysis is useful.

To study the behavior of the damping constant near the dispersion wavelength, we consider the equation:

$$\frac{1}{T} = 1 + \frac{\frac{\gamma d}{c} (\epsilon_{o} - \epsilon_{o})}{\frac{\omega}{\omega} - \frac{\omega}{\omega}} + \frac{\gamma}{\omega}}{(\frac{\omega}{\omega} - \frac{\omega}{\omega})} + \frac{\gamma}{\omega}}$$

The minimum value T_{min} occurs at $\omega = \omega_{o}$

$$\frac{1}{T_{\min}} = 1 + \frac{\frac{\gamma d}{c} (\epsilon_{o} - \epsilon_{\infty})}{(\frac{\gamma}{\omega})^{2}}$$

$$\frac{1}{T_{\min}} - 1 = \frac{\omega^2}{\gamma} \frac{d}{c} (\epsilon_0 - \epsilon_0)$$

and

$$\gamma = \frac{\frac{d}{c} (\epsilon_{o} - \epsilon_{o})}{\frac{1}{T_{min}} - 1} (\frac{2\pi c}{\lambda_{o}})^{2}$$

If the spectra of the same film are recorded at two different temperatures (primed and unprimed) the ratio of γ at these two temperatures will then be:

$$\frac{Y}{Y'} = \frac{\lambda_0'^2}{\lambda_0^2} = \frac{\frac{1}{T'_{\min}} - 1}{\frac{1}{T_{\min}} - 1}$$
 (10)

To make comparisons with other measureable quantities, say

the damping constant at the dispersion wavelength, and the product of the index of refraction n by the extinction coefficient k observed in other experiments, we use the dispersion formula equation (1) and the definition of the dielectric constant to get:

$$n^{2}(1-k^{2} = \epsilon_{\infty} + \frac{(\epsilon_{o} - \epsilon_{\infty})\left[1 - (\frac{\omega}{\omega})^{2}\right]}{\left[1 - (\frac{\omega}{\omega})^{2}\right]^{2} + (\frac{\omega}{\omega})^{2}(\frac{\gamma}{\omega})^{2}}$$

$$2n^{2}k = \frac{\left(\epsilon_{o} - \epsilon_{\infty}\right)\left(\frac{\gamma}{\omega_{o}}\right)\left(\frac{\omega}{\omega_{o}}\right)}{\left[1 - \left(\frac{\omega}{\omega_{o}}\right)^{2}\right]^{2} + \left(\frac{\omega}{\omega_{o}}\right)^{2}\left(\frac{\gamma}{\omega_{o}}\right)^{2}}$$

If we write nk = k and put $\omega = \omega_0$, we get

$$n^2 - k^2 = \epsilon$$

and

$$2nk = \frac{\left(\epsilon_0 - \epsilon_0\right)\omega}{\gamma} = \frac{t}{\gamma}$$

where $(\epsilon_0 - \epsilon_0) \omega_0$ has been written as t for short. Solving these two equations for k^2 we get:

$$k^{2} = -\frac{\epsilon_{\infty}}{2} + \frac{t}{2\gamma} \sqrt{1 + \frac{\gamma^{2} \epsilon_{\infty}^{2}}{t^{2}}}$$

Expanding the square root and neglecting higher order terms we get:

$$k^{2} = -\frac{\epsilon}{2} + \frac{t}{2\gamma} + \frac{1}{4} \epsilon_{\infty}^{2} \frac{\gamma}{t}$$

The dominating term is $\frac{t}{2\gamma}$; upon neglect of the other two terms,

we have

$$k^2 \approx \frac{t}{2\gamma}$$

or

$$nk \sim \sqrt{\frac{(\epsilon_{0} - \epsilon_{0}) \omega}{2\gamma}}$$
 (11)

III. EXPERIMENTAL TECHNIQUE

A. Apparatus

1. Spectrophotometers: Two infrared spectrophotometers are used in the experiment. The first is a Perkin-Elmer double-beam recording spectrophotometer, model 137 ("Infracord") with potassium bromide optics covering the range 12.5 to 25 microns. The second is a Perkin-Elmer double-beam spectrophotometer, model 21 with sodium chloride or cesium-bromide optics, covering the range of 2 to 40 microns. Both spectrophotometers have Nerst glowers as sources, and vacuum thermocouples as detectors.

The model 137 is always used under the same settings, with fixed range, fixed recording speed, and fixed source intensity.

There is only one automatic slit-width program; the slit can be controlled manually, however, if desired. The model 21 is a much more elaborate instrument. Prisms may be interchanged; a sodium-chloride prism is used for the region 2 to 15 microns, and a cesium-bromide prism for the region 15 to 38 microns. For the work reported in this thesis, only the cesium-bromide prism is used.

The slit can be controlled manually, or operated with variable automatic programming. The recording speed and the pen speed can be changed over a wide range. The source intensity and the amplifier gain and damping can be varied to give the desired

sensitivity. The wave length scale of the spectrum can be adjusted by changing the gear ratio. The case can be purged with dry nitrogen gas to minimize the effect of atmospheric absorption.

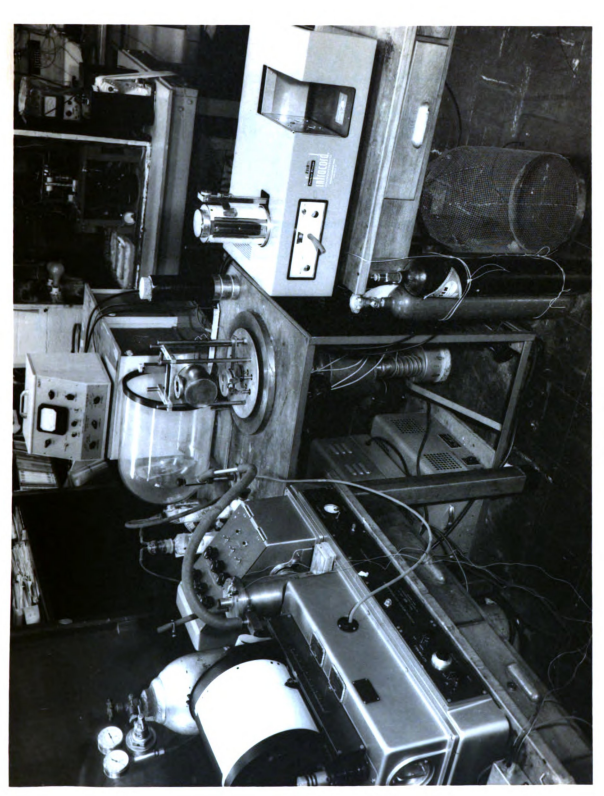
- Evaporator: The evaporator consists of three major parts: A diffusion oil pump, a cylindrical glass bell jar 12 inches in diameter and 18 inches long, and a cylindrical cold trap 14 inches in diameter and 7 inches long. The tube connecting the oil pump to the bell jar is 13/4 inches in diameter. The bell jar sits on a steel circular disc, 16 inches in diameter and 1 inch thick. Eight Kovar-seal leads pass through the plate. A rod that can be rotated from the outside, along with four other fixed rods used to hold the low-temperature cell, passes through the plate into the bell jar. The jar can be evacuated through the fore pump directly, with the diffusion pump shut off from the circuit. When the vacuum is around 25 microns, the bell jar is evacuated through the already hot oil, by the use of three vacuum valves. This procedure brings the pressure down to its lowest value in the shortest time. The vacuum in the evaporator is about 10⁻⁵ mm Hg. Figure 2 shows a general view of the evaporator and the apparatus.
- 3. Low-temperature cell: As shown in Figures 3 and 4, the low-temperature cell consists of an outside cylindrical brass tube 8 1/2 inches long and 4 inches in diameter. A vacuum valve is connected near its top. An inside cylindrical brass tube 4 inches

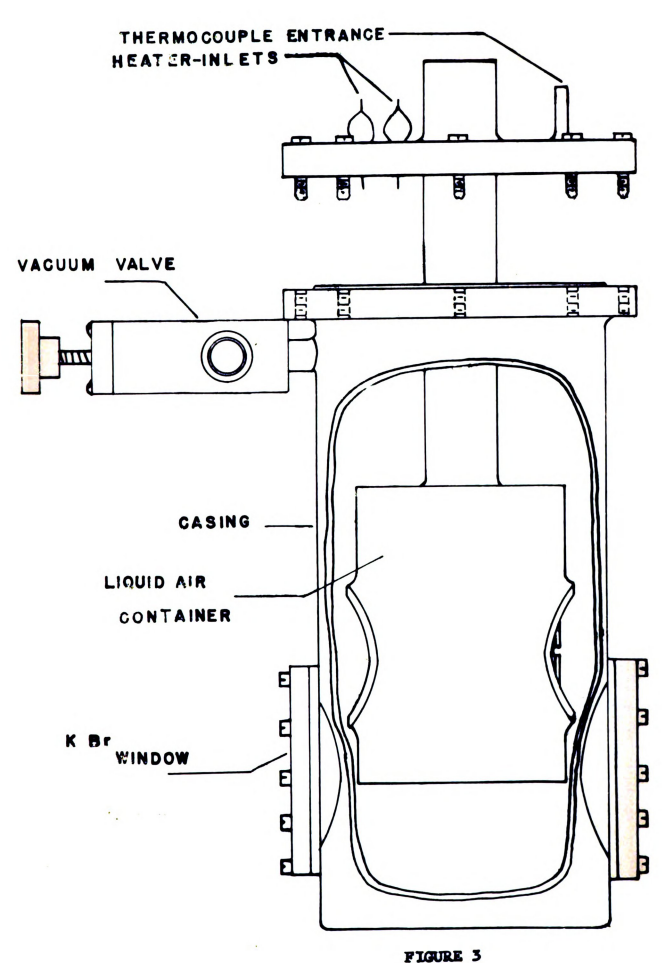
Figure 2. General view of apparatus, showing the evaporator at the center, the Model 137 spectrophotometer to the right, and the Model 21 spectrophotometer to the left.

Figure 3. Cut-away view of the low-temperature sample holder. The inner portion has been raised to clarify details of the cover construction.

Figure 4. Detailed sectional view of the sample holder.

•





long and 3 inches in diameter is connected to a stainless steel tube 6 inches long and 1 1/2 inches in diameter. The openings of the windows on the outside cylinder are 1 1/2 inches in diameter and 1 1/4 inch in diameter, respectively. A brass tube 1 5/8 inches in diameter forms part of the sample holder, being soldered across the inner tube parallel to its base, to be surrounded by the cooling agent from all sides. This tube is threaded across half its length. A second tube threaded along its outer surface fits inside the sample tube, and presses a flat brass ring tight against a shoulder in the middle part of the sample tube. The outside surface of the ring is threaded. In the center is a hole 7/8 inches in diameter with a shoulder where the sample sits, in a pocket containing a heater wire. A cap threaded across its inside surface fits on the disc. To insure good thermal contact between the sample and the sample holder, a small circular copper spring is placed above the sample and is pressed on by the cap. The leads of the thermocouple for measuring the temperatures of the sample and its surroundings are extended inside the cell through a tube on the top plate plugged by a clipped rubber hose which is filled with vacuum grease to prevent air leakage. Two Kovar seals are soldered to the top plate of the cell to provide electrical connections for the heater around the sample. The window holders are designed to permit the use of different kinds of substrate (potassium bromide, polyethylene or cesium

bromide). The window sits on rubber O-rings and is held in place by a brass holder. The cell is designed to operate from liquid-air temperatures to temperatures as high as 400° C. A duplicate cell was built to provide compensation for the reference beam of the spectrophotometers.

B. Film Preparation

LiF. LiF is a stable compound with cubic NaCl structure, melting at 842° C and boiling at 1676° C. Its solubility in water at 18°C is 0.27 gram per 100 grams of water, and at 35°C is 0.135 grams per 100 grams of water. Separated isotopes of lithium in metallic form were supplied by the Oak Ridge National Laboratory. The metal was converted to fluoride by treating it with hydrofluoric acid. Small quantities of powdered fluoride were placed on a boat inside the bell jar of the evaporator. Each boat is made of a molybdenum sheet 3/8 inch wide, 2 inches long, and 0.003 inch thick. The boat is connected to the power supply through two of the Kovar leads. The substrate is placed 4 inches above the boat. Plates of cesium bromide l inch in diameter and 1/8 inch thick, and sheets of polyethylene 1 inch in diameter and 0.040 inch thick are used as substrates. As the powder is set for evaporation, air is pumped out of the bell jar through the fore pumps directly. When the pressure is around 25 microns, the bell jar is evacuated by means of a diffusion pump. The pressure drops to around 10⁻⁴ mm in about 5 minutes. The boat is heated slightly for a few minutes, allowing it along with the powder to outgas. The current is now raised until the powder melts and evaporates. If an attempt is made to evaporate it without outgassing, it hops off the boat. During the early part of the evaporation, an aluminum shutter screens the substrate to prevent deposition of readily volatile impurities. The evaporation is continued until the films are of the order of 0.01 to 0.10 microns thick.

Films containing varying compositions of Li⁶F¹⁹ and Li⁷F¹⁹ are also evaporated. Samples of the different compositions were prepared using a precision balance and processed just like the isotopically-pure specimens.

2. LiH: LiH is a reactive compound with cubic NaCl structure, melting at 680°C. It has a density of 0.780 ± 0.007 gm/cm³ at 20°C. It reacts vigorously if it comes in contact with water, liberating hydrogen gas and leaving lithium hydroxide as residue. It also reacts with humid air to form a coating of lithium hydroxide and lithium carbonate. At 200°C, LiH reacts even with dry air.

LiH and LiD samples were obtained in powder form from the Foote Mineral Company and from Metal Hydrides, Incorporated,

respectively. The approximate analysis by weight as supplied by the manufacturers is as follows:

Li⁶ H¹ and Li⁶ H² were obtained in lump form from the Stable Isotopes Research and Production Division of Oak Ridge National Laboratory.

The manufacturer reports the following analysis for the samples:

Li H	Grams lithium per	gram material:
	Experimental	Calculated
	0.8470	0.8574

Spectrographic analysis.*

Element	Weight percent	
Na	0.28	
Ca	**<0.004	
K	<0.004	
Ag	0.0004	
Cu	0.001	
Mg	0.002	
Mn	0.004	
Mo	<0.0004	

^{*}The spectrographic results reported herein are semi-quantitave estimates and should not be interpreted or construed to be precise quantitative determinations.

^{**}No spectrum line visible; probably absent; definitely less than value given.

Element	Weight percent
Al	0.003
В	<0.002
Ba	0.004
Be	<0.0002
Cd	<0.0006
Со	<0.002
Cr	<0.0001
Ni	0.006
Pb	0.001
Si	0.004
Sn	<0.0002
Sr	<0.001
V	<0.001
Zn	<0.1
Nb	<0.1
, 6 _L 2	
7; "LI"	Chama lithium non a

Li⁶H² Grams lithium per gram material:
Experimental Calculated

0.7473 0.7527

Spectrographic analysis:

Element	Weight percent
Na	<0.004
Ca	<0.004
K	0.004
Ag	0.001
Al	0.002
В	<0.002
Ba	0.002
Be	<0.0002
Pb	0.0008
Si	0.002
Sn	<0.002
Sr	<0.001
Cd	<0.0006
Co	<0.002
Cr	0.0001

Element	Weight percent
Cu	0. 0015
Mg	0.002
Mn	0.0002
Mo	<0.004
Ni	0.006
V	<0.001
Zn	<0.1
Nb	<0.001

Thin films of LiH if exposed to air with the least amount of humidity will suffer an immediate chemical transformation to lithium hydroxide and other compounds of lithium. To overcome this difficulty, the low-temperature cell described earlier in this chapter was constructed. The cell is designed to fit inside the bell jar of the evaporator and to hold the sample after it is evaporated. The cell is then taken out of the bell jar and placed in the spectrophotometer while vacuum is maintained in its interior. An aluminum bracket is designed to hold the cell horizontally on the four fixed rods above the plate. The larger window opening on the cell is situated above the molybdenum boat. The movable rod holds the window of the cell. The window sits in an aluminum holder resting on a spring that equalizes the pressure on the window when it is pressed against the O-ring. The holder is covered by an aluminum cover which carries two small magnets on its top to permit raising it with a steel bar. The molybdenum boat is held by two brass pieces soldered to two flexible wires. The wires are connected to two of the Kovar seals

supplying the power. The flexibility of the wires allows for the adjustment of the height of the boat and for the removal of the boat after evaporation.

The boat is placed partially inside the window opening to prevent as much as possible the O-ring from being coated by the hydride. An aluminum foil shield covers the window opening and is taped to the movable bar in order to prevent the first part of the evaporation from reaching the substrate. The LiH powder is stored in a large bottle and a portion transferred through the atmosphere to a small weighing bottle for use. The transfer takes about five seconds; about ten or fifteen more seconds is needed to transfer LiH from the weighing bottle to the boat. Thus the evaporated LiH is exposed to the atmosphere for 15 to 20 seconds prior to its evaporation. It is likely then that a layer of hydroxide is already created on the hydride before it is evaporated. Since LiOH melts at 450 °C, it is hoped that the aluminum shield prevents the LiOH from reaching the sample substrate after it is evaporated. When the pressure inside the evaporator is around 10⁻⁴ mm Hg, hydrogen gas is leaked into the evaporator which raises the pressure up to about 2×10^{-3} mm Hg. The evaporation of the LiH films then takes place in a hydrogen atmosphere. A small current is passed through the molybdenum boat, allowing both the boat and the powder to outgas. The current is increased slowly until the powder starts melting. The first portion

of the evaporation is screened off by the aluminum shield. The shield is then removed and the LiH strikes the film substrate. The thickness of the film is judged by observing a light beam reflected through the film and the substrate. The boat is knocked down by the window holder and the cover is removed by the use of the two magnets. The window holder is rotated and pressed gently in its position against the O-ring. Air is allowed to fill the bell jar. The difference between the atmospheric pressure and the pressure inside the cell seals the window tight in its position, preserving the vacuum in the interior of the cell. The cell is taken out, freed from the aluminum bracket and placed into the spectrophotometer. A hose connects the cell to the evaporator, and the cell is pumped on through the entire experiment to maintain a constant vacuum in the interior of the cell. The thickness of the evaporated films is of the order of 0.01 to 0.1 microns. Films of varying compositions of LiH and LiD were also evaporated. The different compositions were weighed and mixed in a dry box.

C. Temperature Measurement

A Daystrom-Weston multiple-station self-balancing recording potentiometer and copper-constantan thermocouples with teflon-fiber glass insulation, 36 gauge, are used to measure the temperature. The temperature is measured at two positions, in the sample substrate and in the brass around the substrate. One of the thermocouple junctions

drying plastic cement to insure good thermal contact between the junction and the sample substrate. The second thermocouple junction is held tight between the sample holder and shoulder where the holder is fastened tightly. The thermocouple wires enter the interior of the cell through the tightly clipped rubber hose filled with vacuum grease and plugging the tube on the top plate of the cell.

IV. EXPERIMENTAL RESULTS

A. Lithium Fluoride

All the work on LiF is done with the Perkin-Elmer Model 21

Spectrophotometer in the region of the spectrum from 15 to 40 microns.

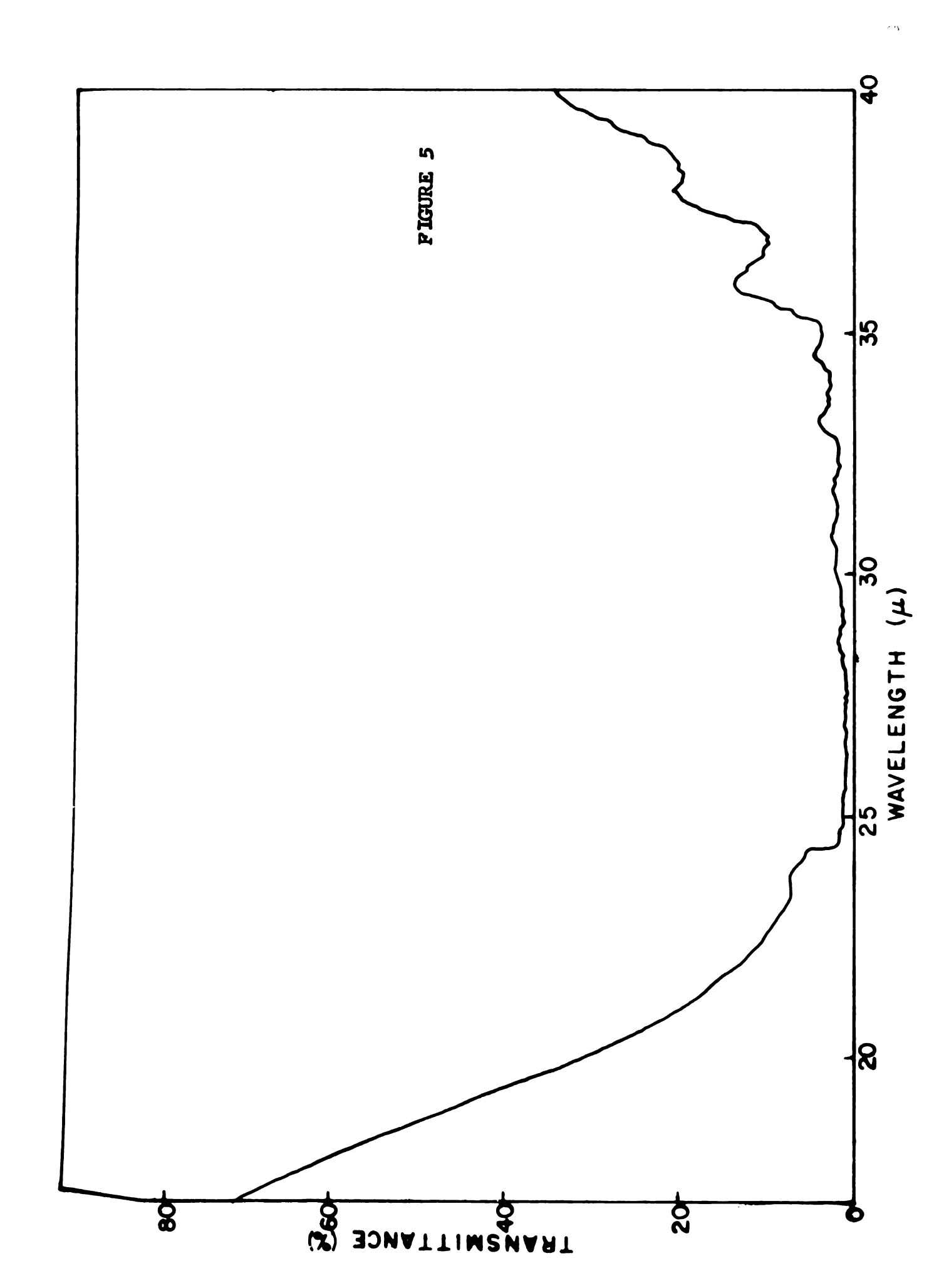
The region of the spectrum from 24 to 40 microns is greatly influenced by water and carbon-dioxide absorption bands, as seen in figure 5.

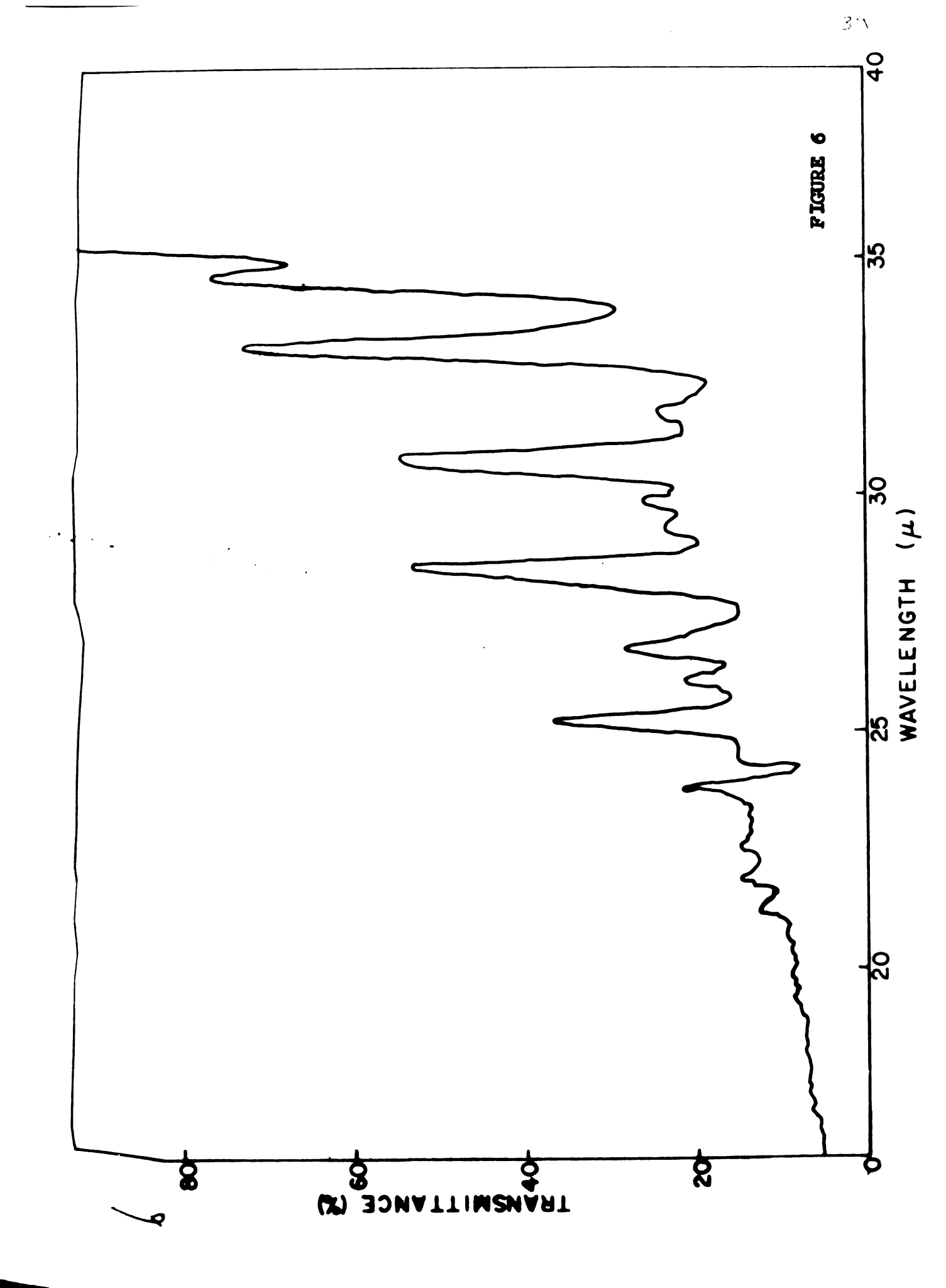
Figure 6 shows the result of a stray-radiation run, wherein the sample beam is covered by a thick NaCl plate to absorb all radiation beyond say 20 microns. For some spectra, the sample compartment was covered tightly with aluminum foil and the instrument was flushed with dry nitrogen gas in an attempt to reduce the effect of atmospheric absorption. This procedure led to a reduction in the intensity of the atmospheric bands, but they remained strong enough to continue to change the shape of the LiF spectra. Throughout the entire work on LiF, polyethylene windows were used on the low-temperature cell.

- 1. Effect of isotopic mass--Li 6 F¹⁹, Li 7 F¹⁹: The dispersion wavelength for Li 6 F¹⁹ evaporated as a thin film on a sheet of polyethylene is 30.8 $^+$ 0.1 microns, and that for Li 7 F¹⁹ is 32.5 $^+$ 0.1 microns. This finding is in agreement with the previous results found by Montgomery and Misho (12).
- 2. <u>Effect of isotopic composition</u> -- [xLi⁶, (1-x)Li⁷] F¹⁹: Figures 7 to 17 show the spectra for the various compositions

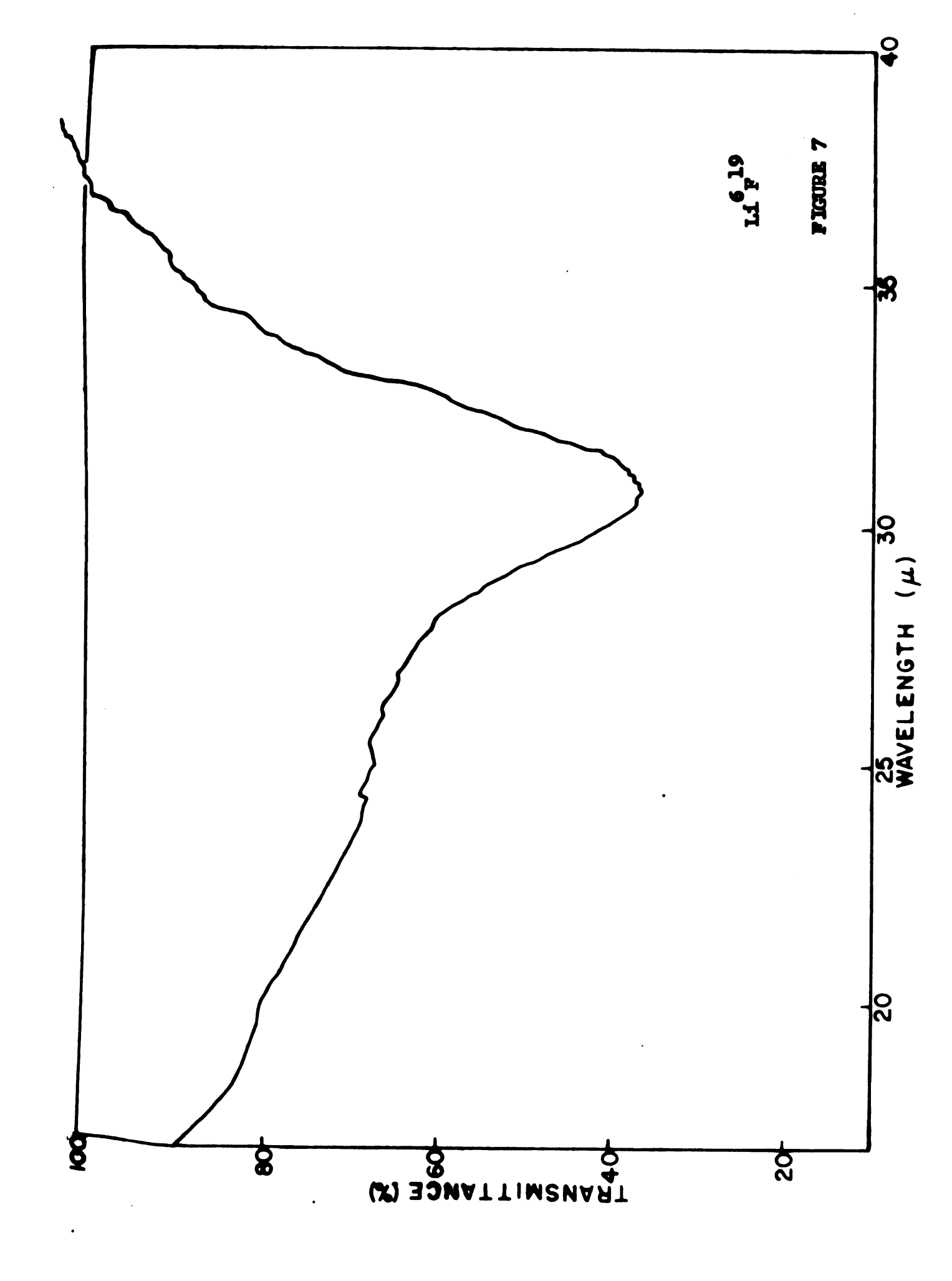
Figure 5. Stray-radiation run: The sample slit has been covered with a thick sodium-chloride plate to absorb radiation of longer wavelengths. The transmitted intensity drops gradually past 15μ , falling sharply at 24.5 μ , where a reststrahlen filter is inserted in the optical path. From 25 μ to 32 μ or so, a negligible proportion of stray radiation reaches the detector. Then scattered radiation from the short-wavelength region (transmitted through sodium-chloride shutter) becomes significant.

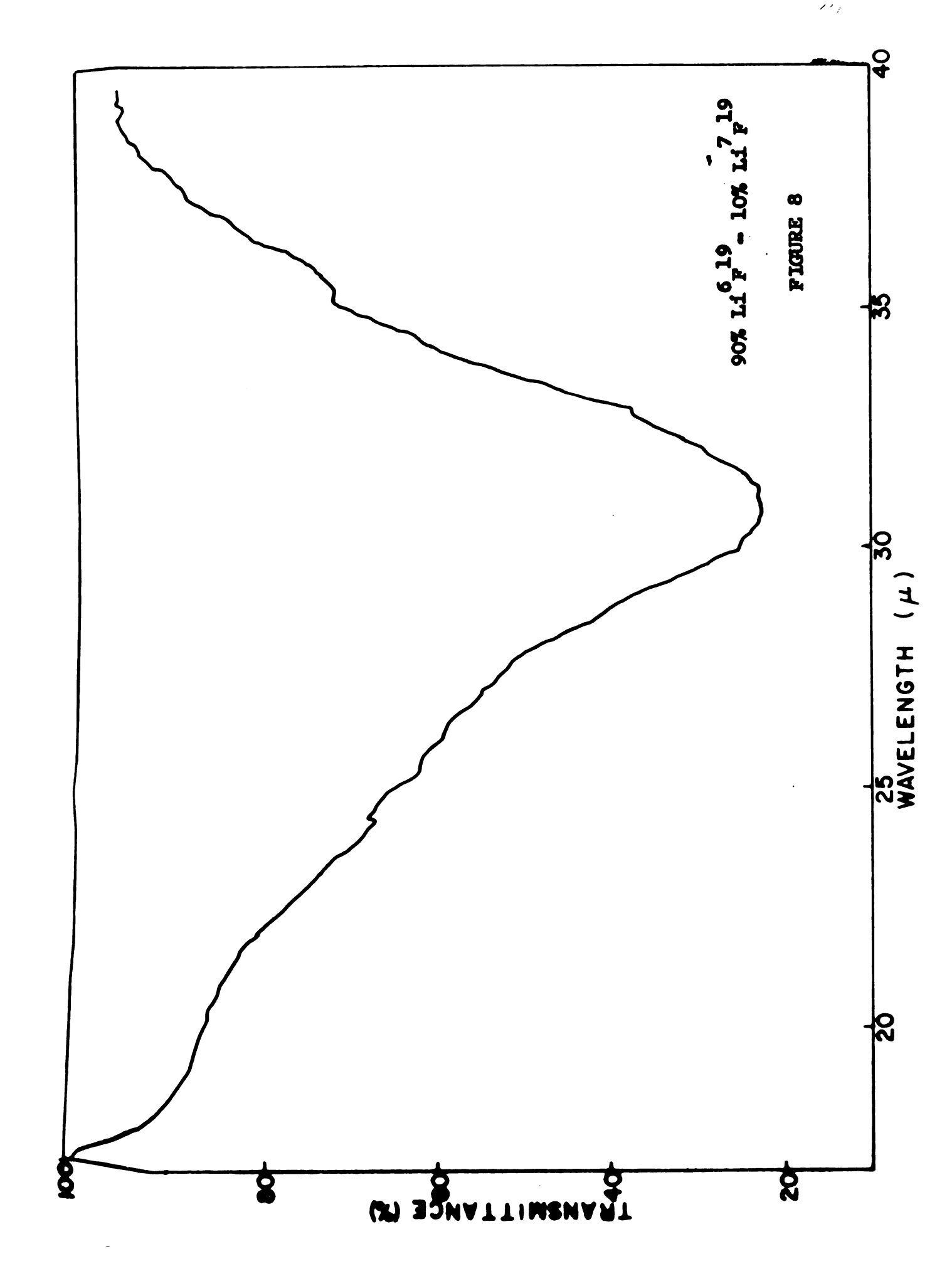
Figure 6. Atmospheric-absorption run: The sample slit has been covered with an opaque shutter, and a fixed signal has been injected into the detector input circuit. The reference-beam shutter then opens to the amount necessary to compensate for the injected signal. The peaks are due to well-known water-vapor and carbon-dioxide bands, and can be used to calibrate the instrument.

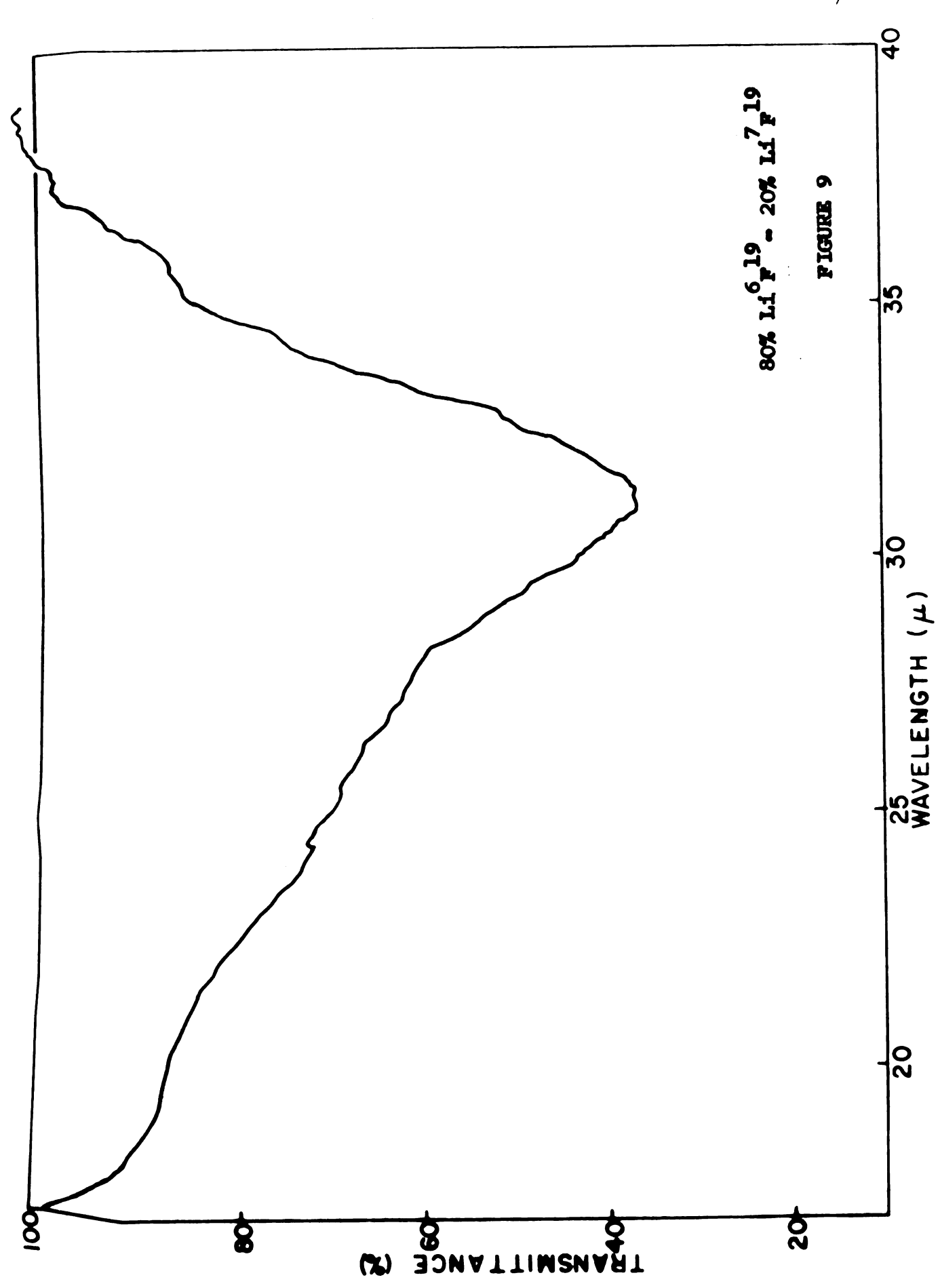


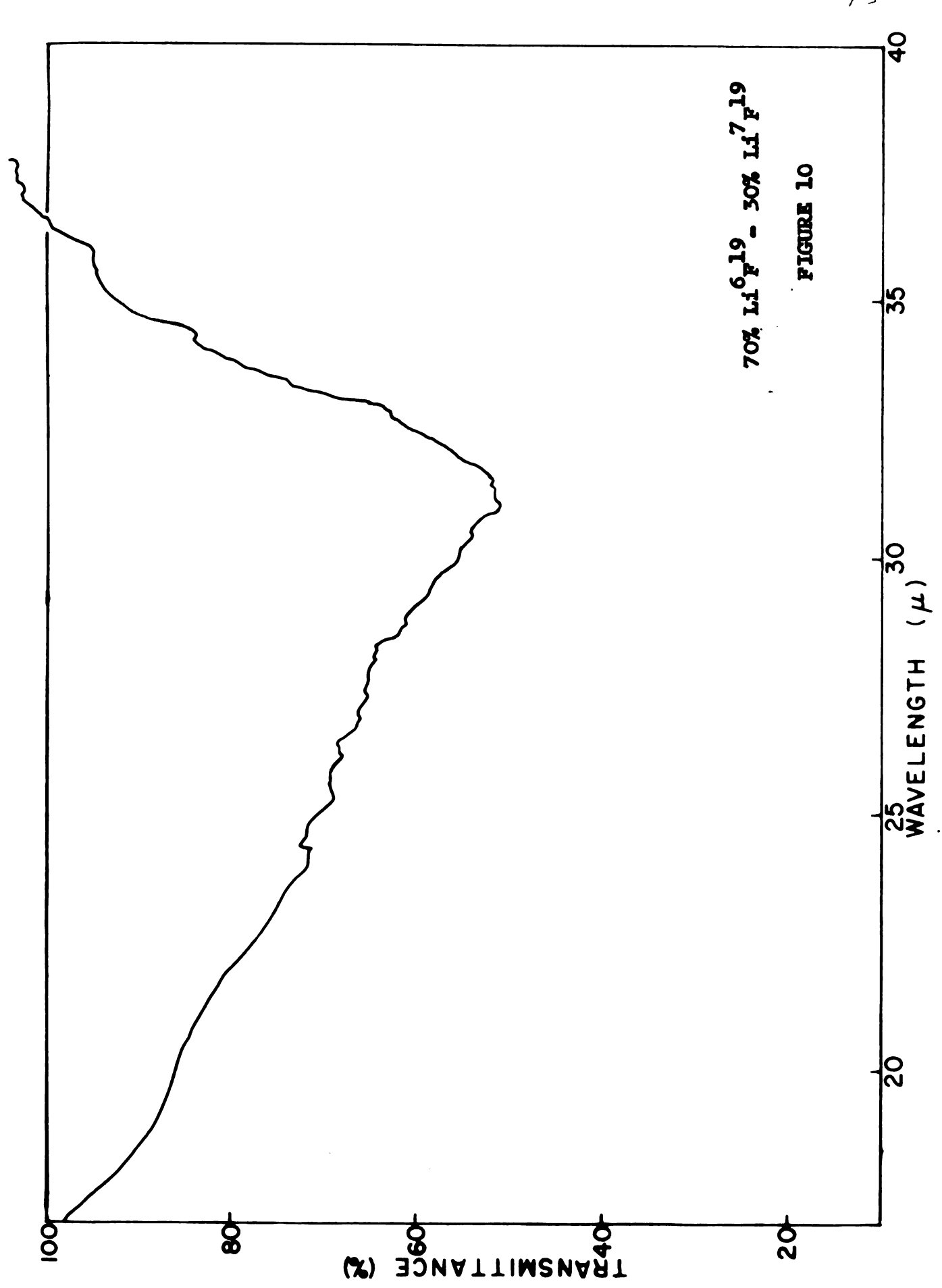


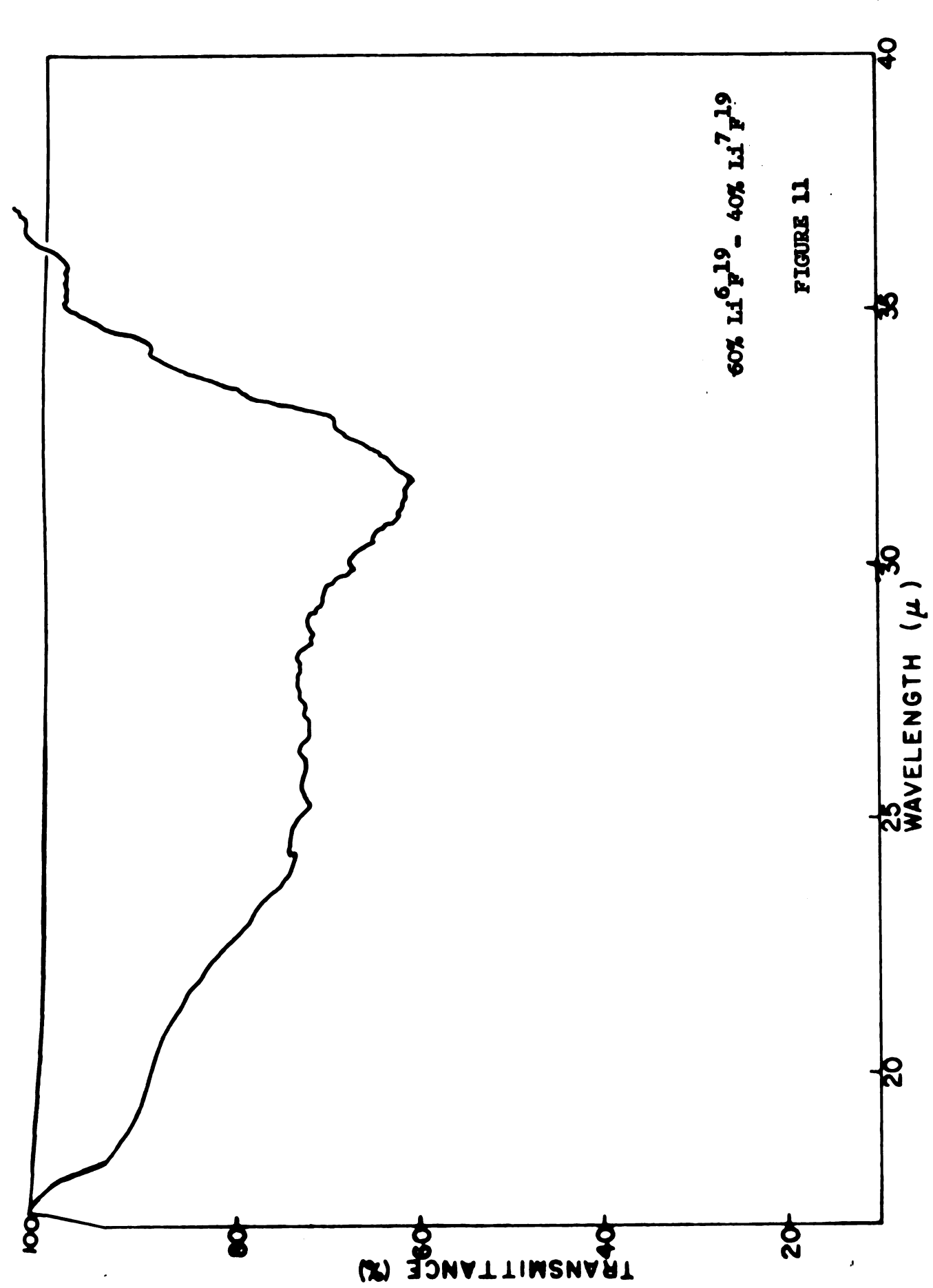
Figures 7-17. Infrared absorption spectra of thin films of LiF¹⁹ containing varying proportions of Li⁶F¹⁹ and Li⁷F¹⁹ as indicated on individual figures. Temperature, 300°K; substrate, polyethylene sheet.

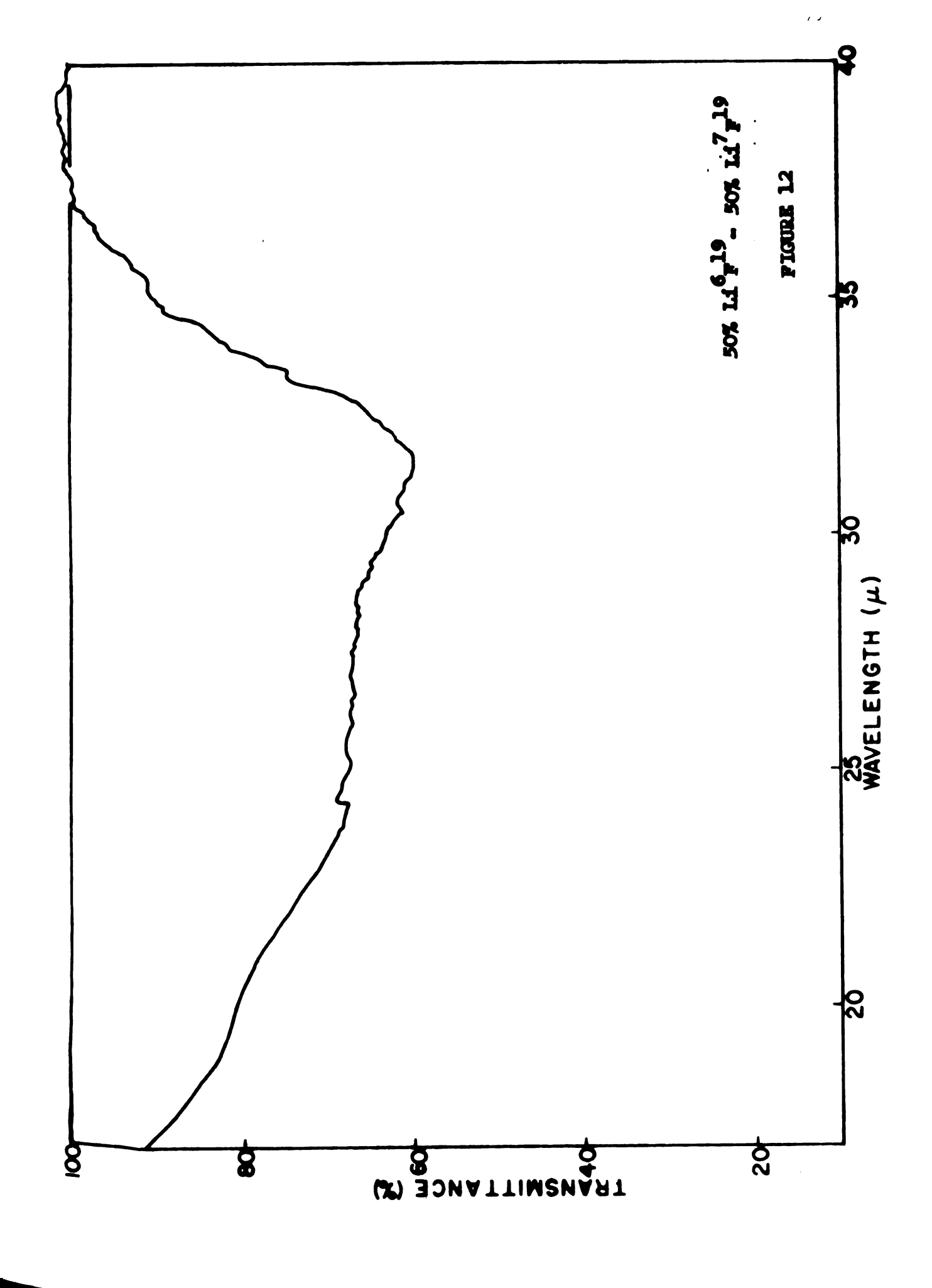


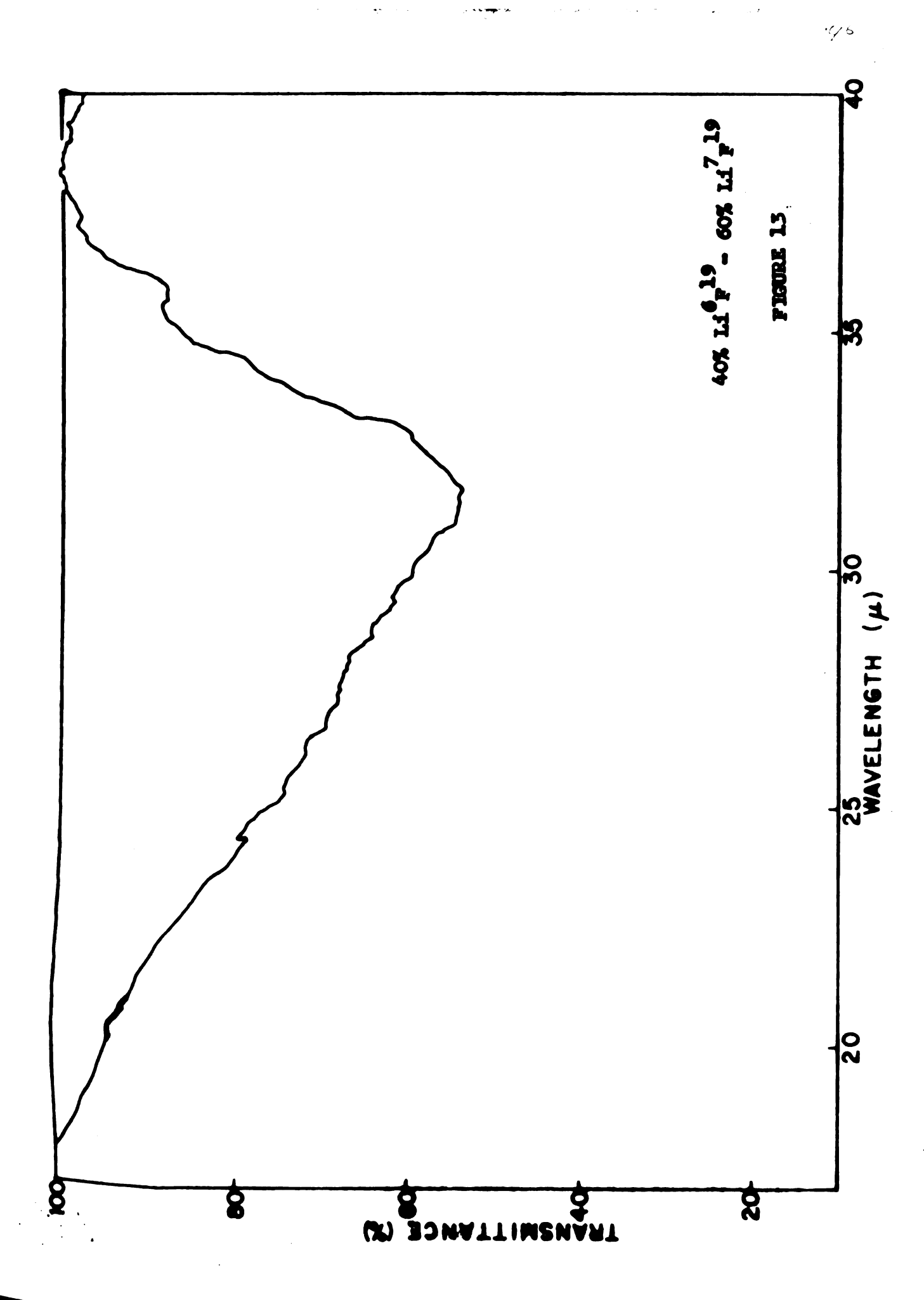


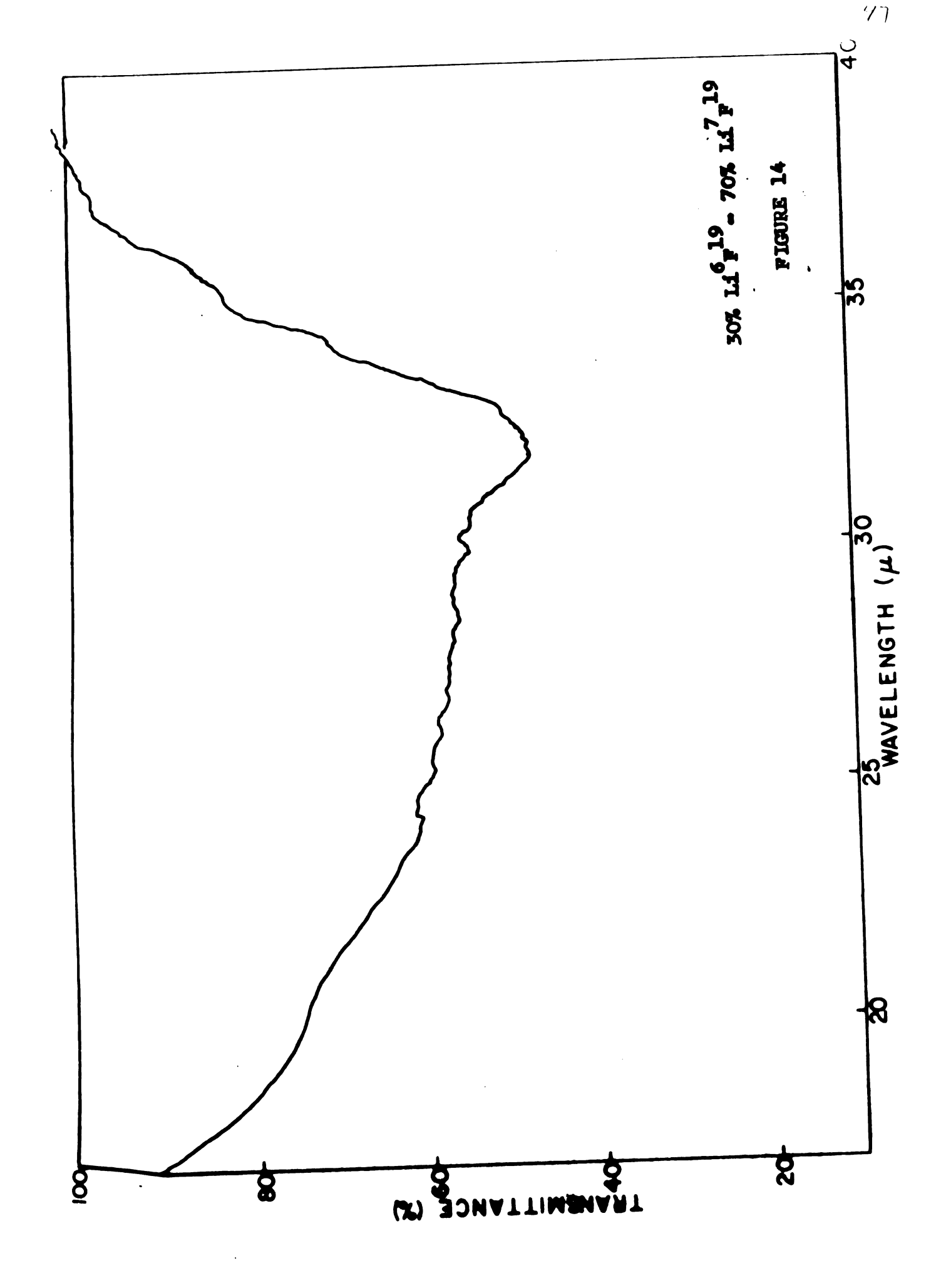


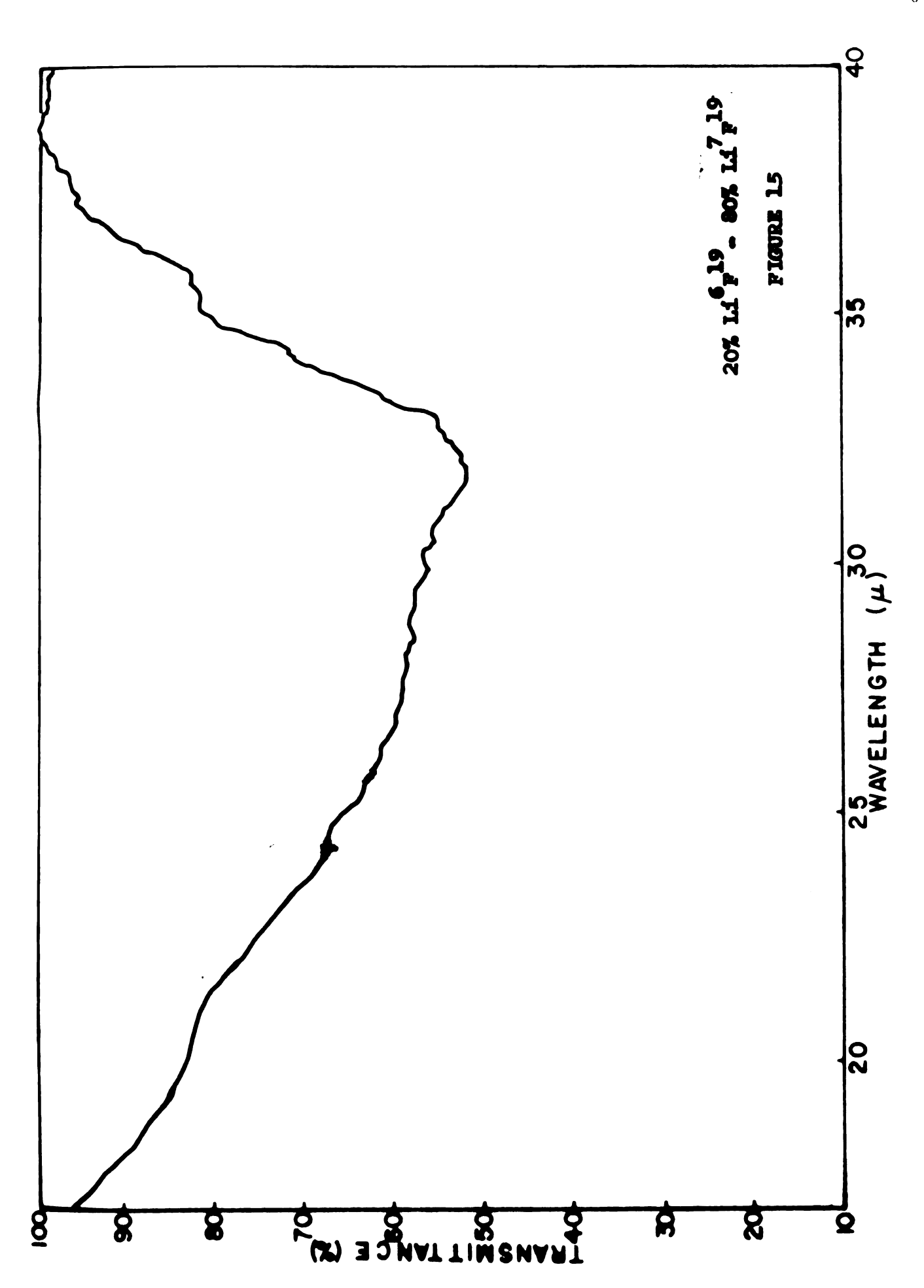


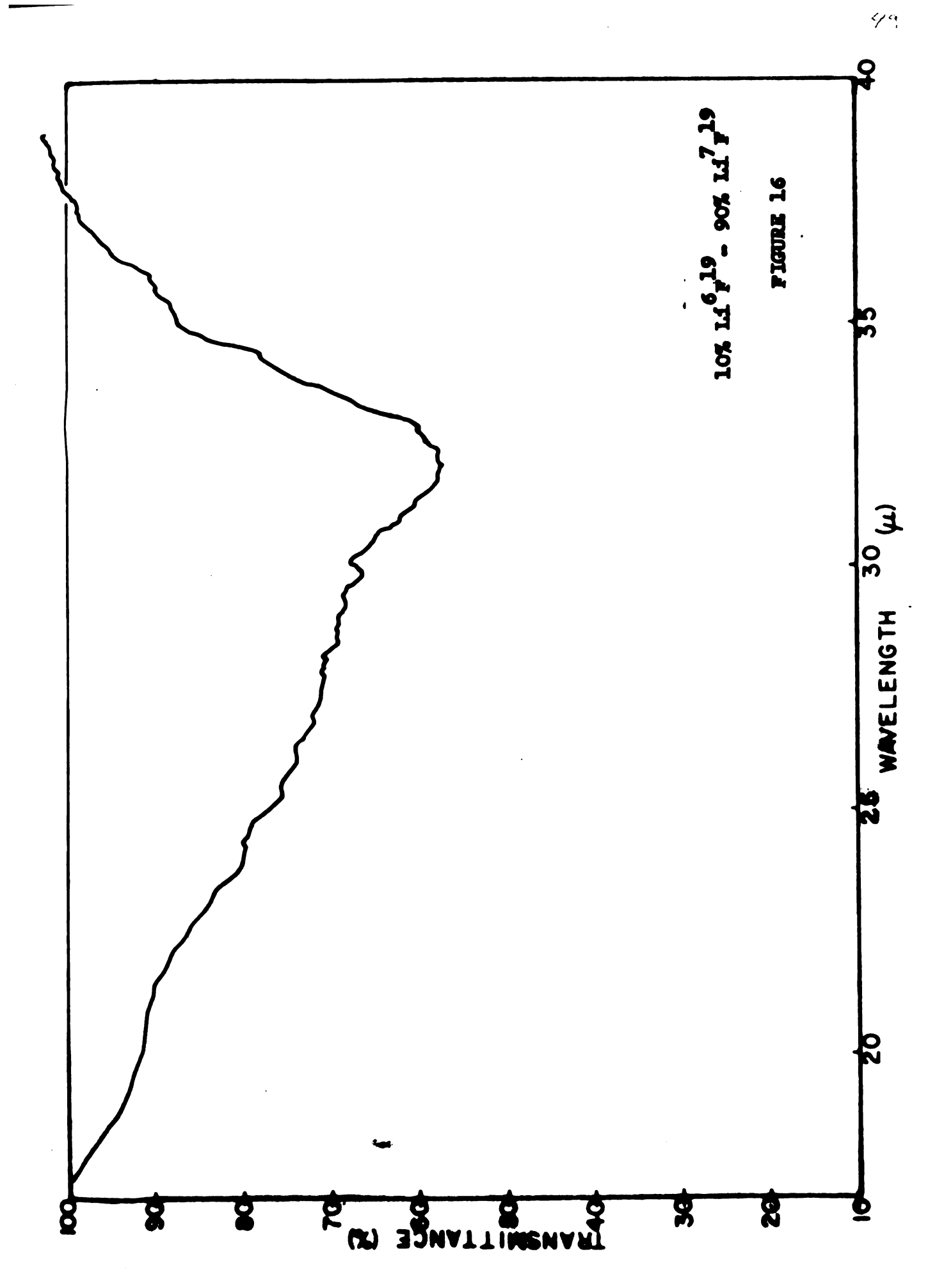


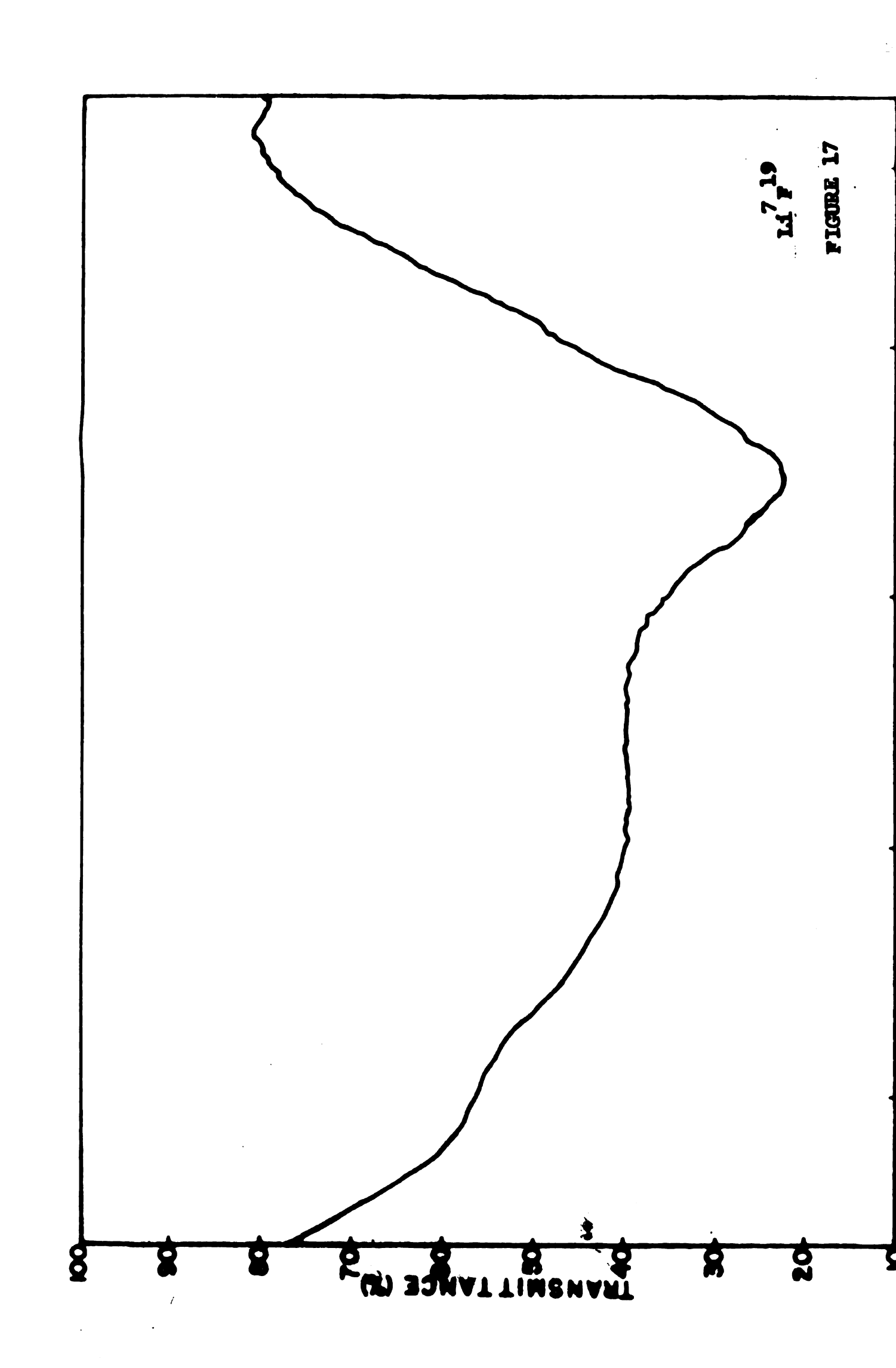












evaporated on polyethylene and recorded at 300°K. For these spectra, the sample compartment of the spectraphotometer was tightly covered with aluminum foil, the recorder pen was set at its lowest speed, the amplifier gain set at its highest value, and the spectra were recorded at slow speed. The various compositions and their reduced masses are listed in Table I. The results at room temperature are in agreement with the results found earlier in reference (12).

- 3. Effect of temperature: At low temperature, the dispersion wavelengths of the pure Li⁶F¹⁹ and Li⁷F¹⁹ films, and of the films made from their various compositions, shift towards shorter wavelengths. Their absorption spectrum becomes deeper and narrower. The average amount of the shift in the dispersion wavelength of films evaporated on the polyethylene substrate at 120°K and 200°K is 1. 3 and 0.5 microns respectively. The average shift for films evaporated on CsBr substrates is 1.2 microns. Typical spectra of films evaporated on polyethylene sheets, as recorded at 300°K, 200°K and 120°K, are shown in Figures 18 through 21.
- 4. Effect of substrate, polyethylene, CsBr: It is found that the position of the dispersion wavelength varies to some extent with the different substrates. As mentioned earlier, polyethylene discs l inch in diameter and 0.040 inch thick, and CsBr plates l inch in diameter and 0.125 inch thick, were used as substrates for the thin films of LiF. There appears to be about 0.2 micron difference

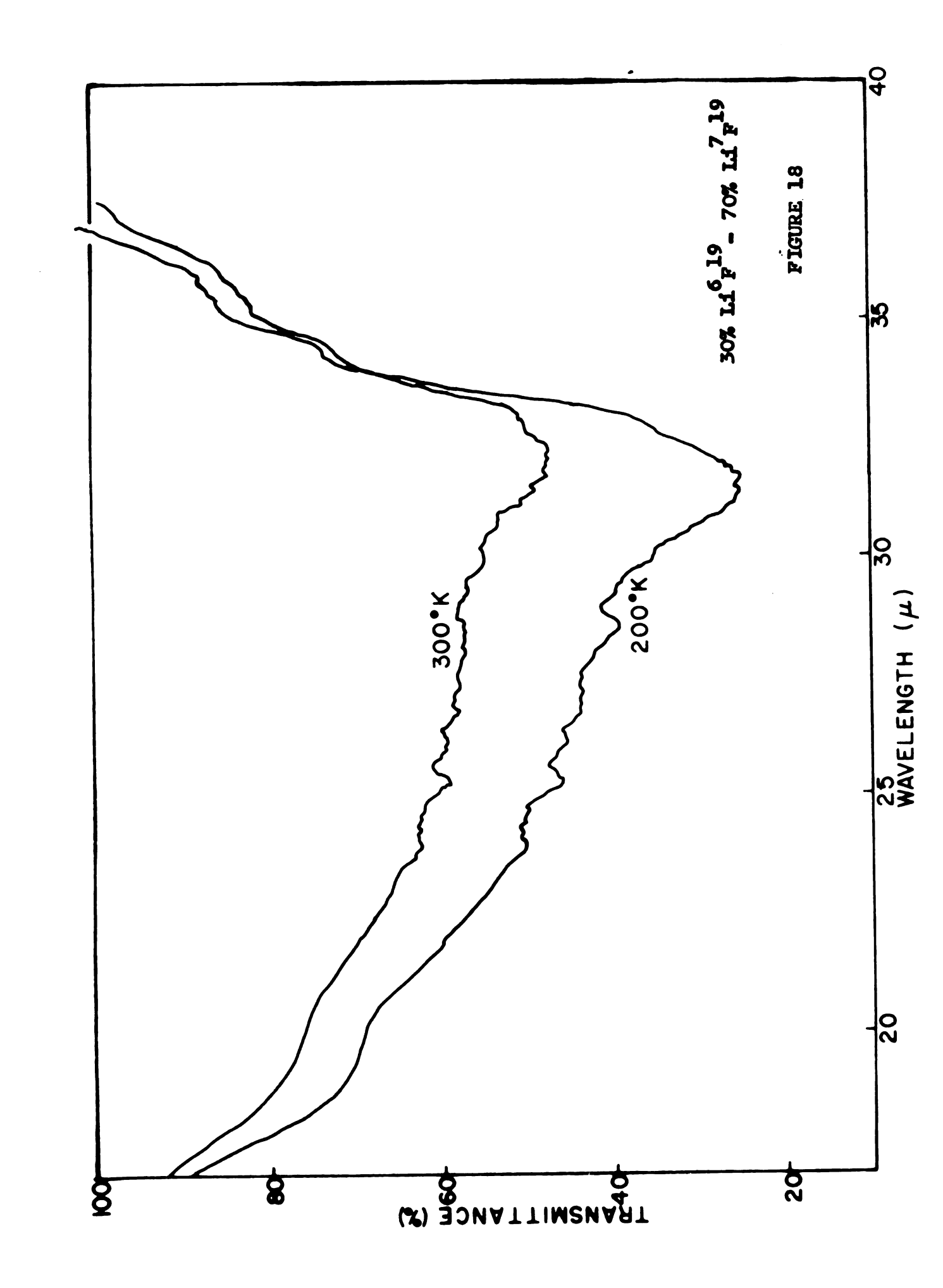
TABLE (1). Reduced masses

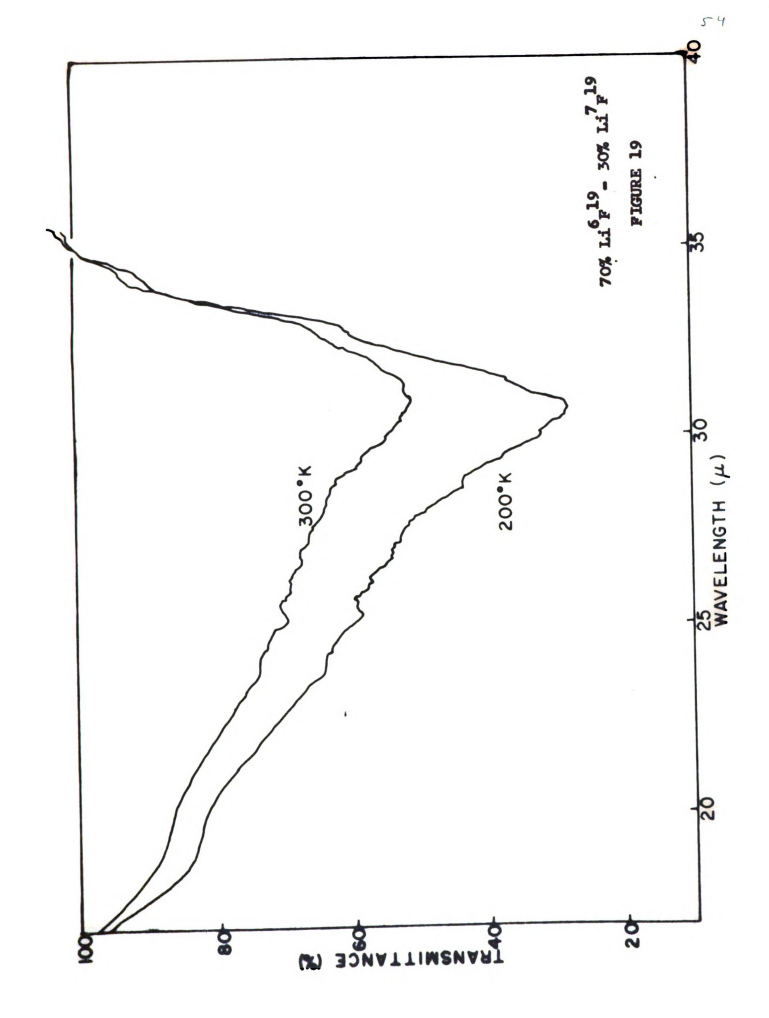
%Li ⁶ F ¹⁹	%Li ⁷ F ¹⁹	μχ	μ x /μs
100	0	4. 570	0.941
90	0	4.633	0.951
80	20	4.695	0.957
70	30	4.755	0.963
60	40	4.813	0.969
50	50	4. 869	0.975
40	60	4.924	0.980
30	70	4.976	0.985
20	80	4.027	0.990
10	90	4.077	0.995
0	100	5. 125	1.000

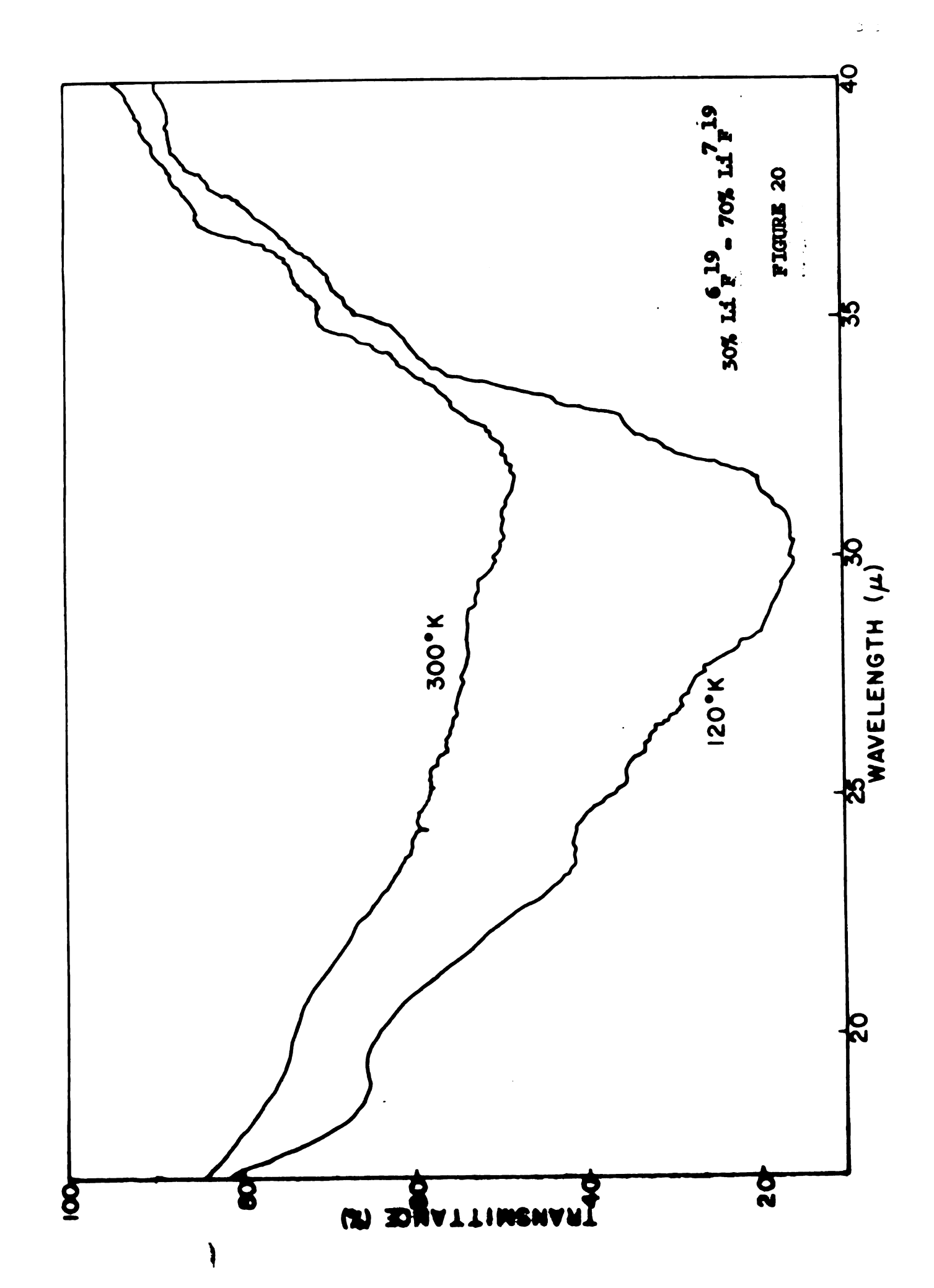
 $[\]mu_{s} = 5.125$

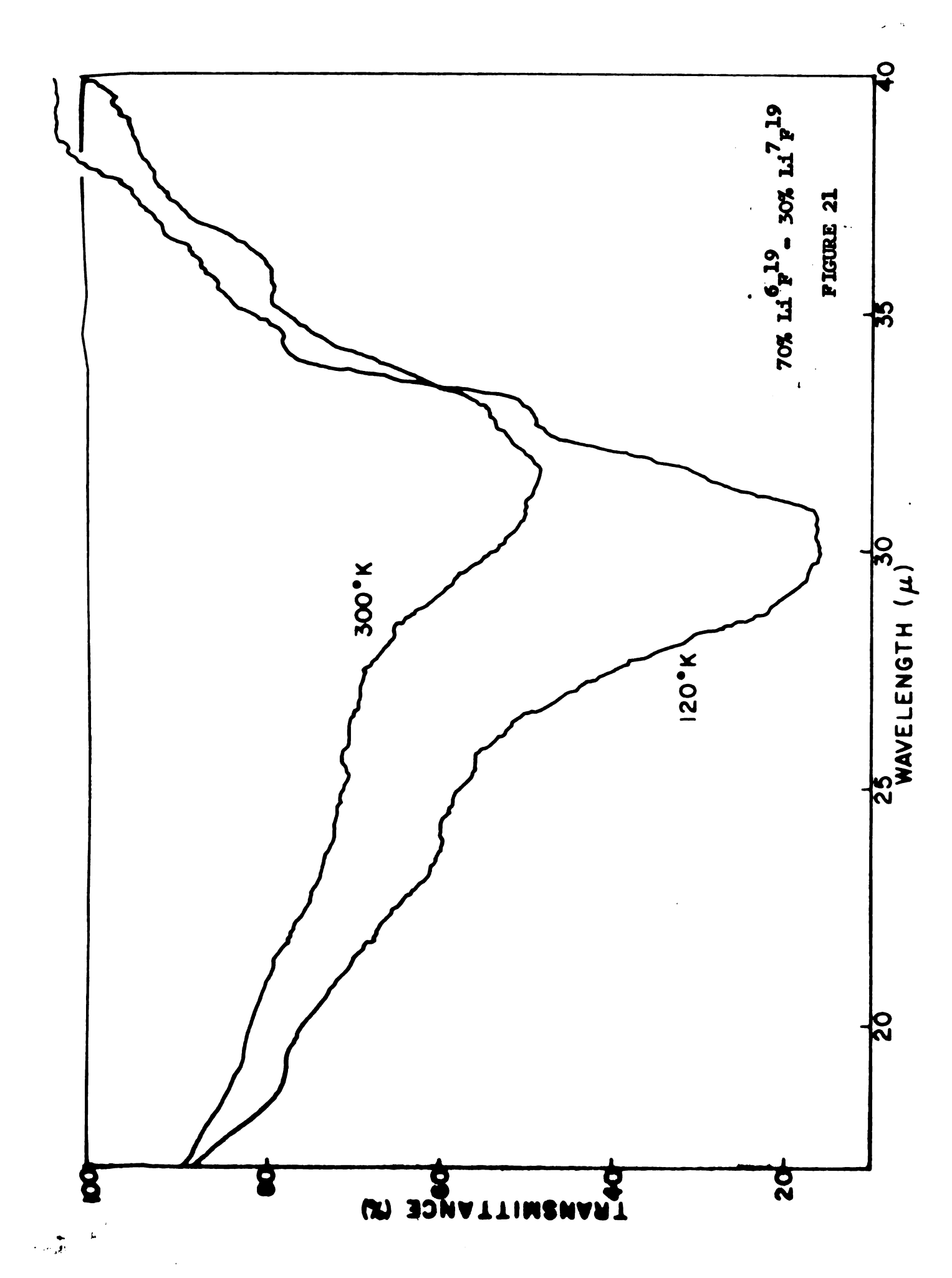
Figures 18-19. Infrared absorption spectra of thin films of LiF¹⁹ containing 30% Li⁶F - 70% Li⁷F (Figure 18) and 70% Li⁶F - 30% Li⁷F (Figure 19). Temperatures, 300°K and 200°K; substrate, polyethylene.

Figures 20-21. Infrared absorption spectra of thin films of LiF¹⁹ containing 30% Li⁶F - 70% Li⁷F (Figure 20) and 30% Li⁶F - 70% Li⁷F (Figure 21). Temperatures, 300°K and 120°K; substrate, polyethylene.







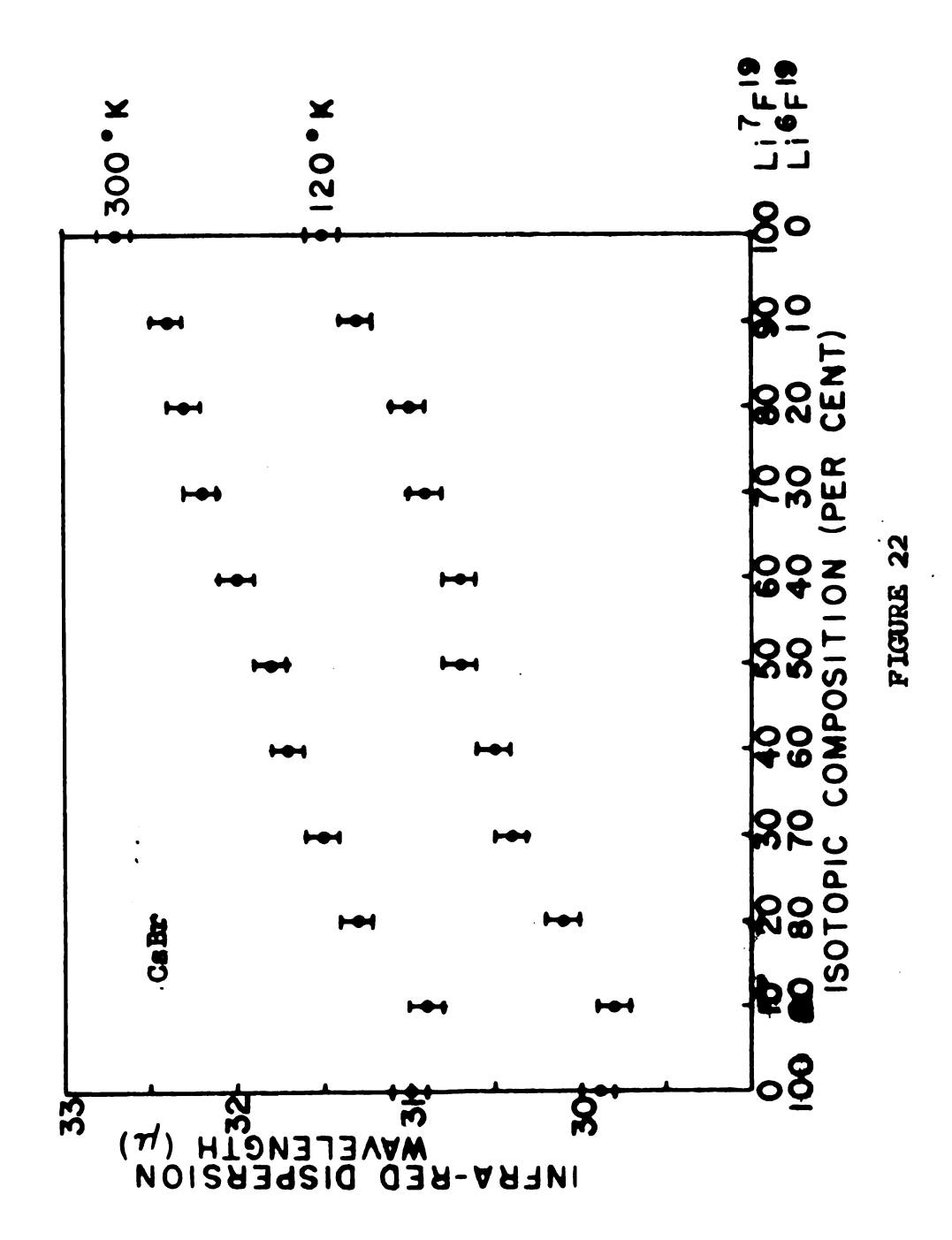


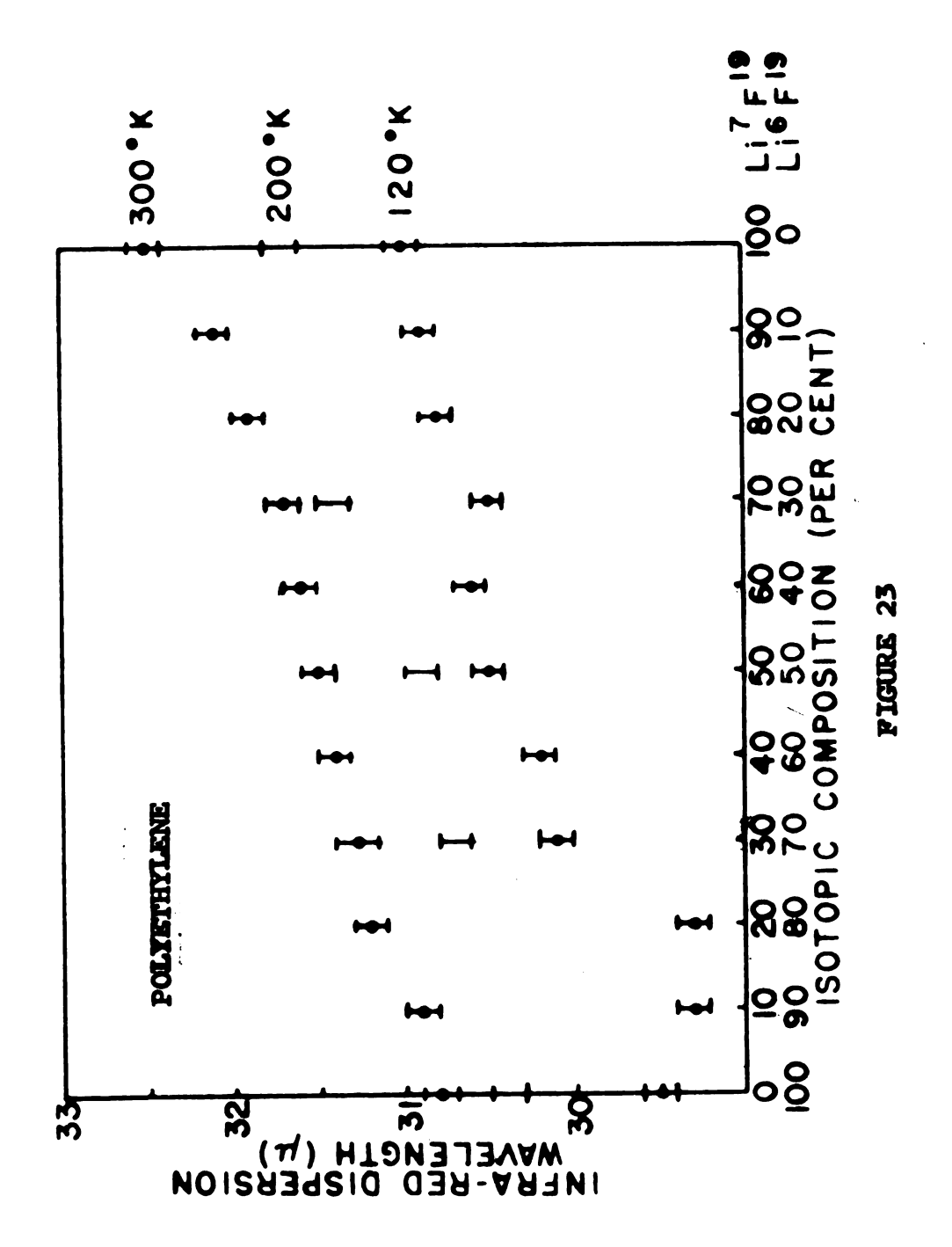
between the dispersion wavelength of films evaporated on polyethylene and those of the same compositions evaporated on CsBr substrates. Films evaporated on CsBr plates have the longer dispersion wavelength. This effect is shown in Figures 22 and 23. Figure 22 shows the variations of the dispersion wavelength with the various compositions of Li ⁶ F ¹⁹ and Li ⁷ F ¹⁹ evaporated on polyethylene and recorded at 300°K, 200°K and 120°K. Figure 23 shows the variations of the various compositions evaporated on CsBr and recorded at 300°K and 120°K.

in this chapter, the spectrum due to the atmospheric absorption interferes with the LiF spectrum. To obtain the net spectra the atmospheric effects are subtracted from the original LiF spectra. The stray radiation that starts to become relatively important at 35 microns and higher owing to the drop in the absolute spectral intensity of the source is also subtracted in part from the original LiF spectra. Two auxiliary minima appear on the short wavelength side of the LiF spectrum. The first peak is around 18 microns, the second is around 25 microns. These minima are shallow and hard to distinguish, but they may be separated from the main absorption peak as follows: The whole spectrum is first corrected for the atmospheric effects and stray radiation. Then, with the help of the equation $\lambda_+\lambda_-=\lambda_0^2$, where λ_0 can be estimated to within $\frac{+}{-}$ 0.1 or better, the

Figure 22. Infrared dispersion wavelength for LiF¹⁹ films evaporated onto sesium-bromide substrate, as a function of isotopic composition x. Temperature: 300° K and 120° K.

Figure 23. Infrared dispersion wavelength for LiF¹⁹ films evaporated onto polyethylene substrate, as a function of isotopic composition x. Temperatures: 300°K, 200°K, and 120°K.





short wavelength side of the main absorption peak is constructed from the long wavelength side of the main absorption peak. The constructed short-wavelength side is then subtracted from the main portion of the spectrum at the corresponding wavelengths. The result is the separation of the auxiliary minimum near the main peak. The second auxiliary minimum is separated by the same procedure. Figure 24 shows the separation procedure as applied to a spectrum of Li $^6F^{19}$ film evaporated on polyethylene, and recorded at $200^{\circ}K$.

6. Evaluation of γ/ω_0 : Equation (9) is used to calculate γ/ω_0 at 300° K. Table 2 lists these values for the spectra shown in Figures 7 through 17. Equation (10) is used to find γ/γ' and γ/γ'' for the spectra shown in Figures 18 through 21, where γ is the damping constant at 300° K, γ' at 120° K and γ'' at 200° K. These values are shown below:

$$\frac{\gamma/\gamma'}{30\% \text{ Li}^{6} \text{F}^{19}, 70\% \text{ Li}^{7} \text{F}^{19}} \qquad 4.1 \qquad 2.3$$

$$70\% \text{ Li}^{6} \text{F}^{19}, 30\% \text{ Li}^{7} \text{F}^{19} \qquad 4.1 \qquad 2.4$$

Unfortunately the parameter γ/ω_0 is highly sensitive to interference by atmospheric absorption and instrumental noise, and it can be determined with meaning only by great expenditure of time and care. Consequently this parameter was determined on one substrate (polyethylene) for all compositions at room temperature only and for selected compositions at low temperature and on the same substrate.

Figure 24. Separation of main absorption peak from minor ones, for spectrum of ${\rm Li}^6 {\rm F}^{19}$ film deposited onto polyethylene substrate. Temperature: 200 $^{\rm O}$ K.

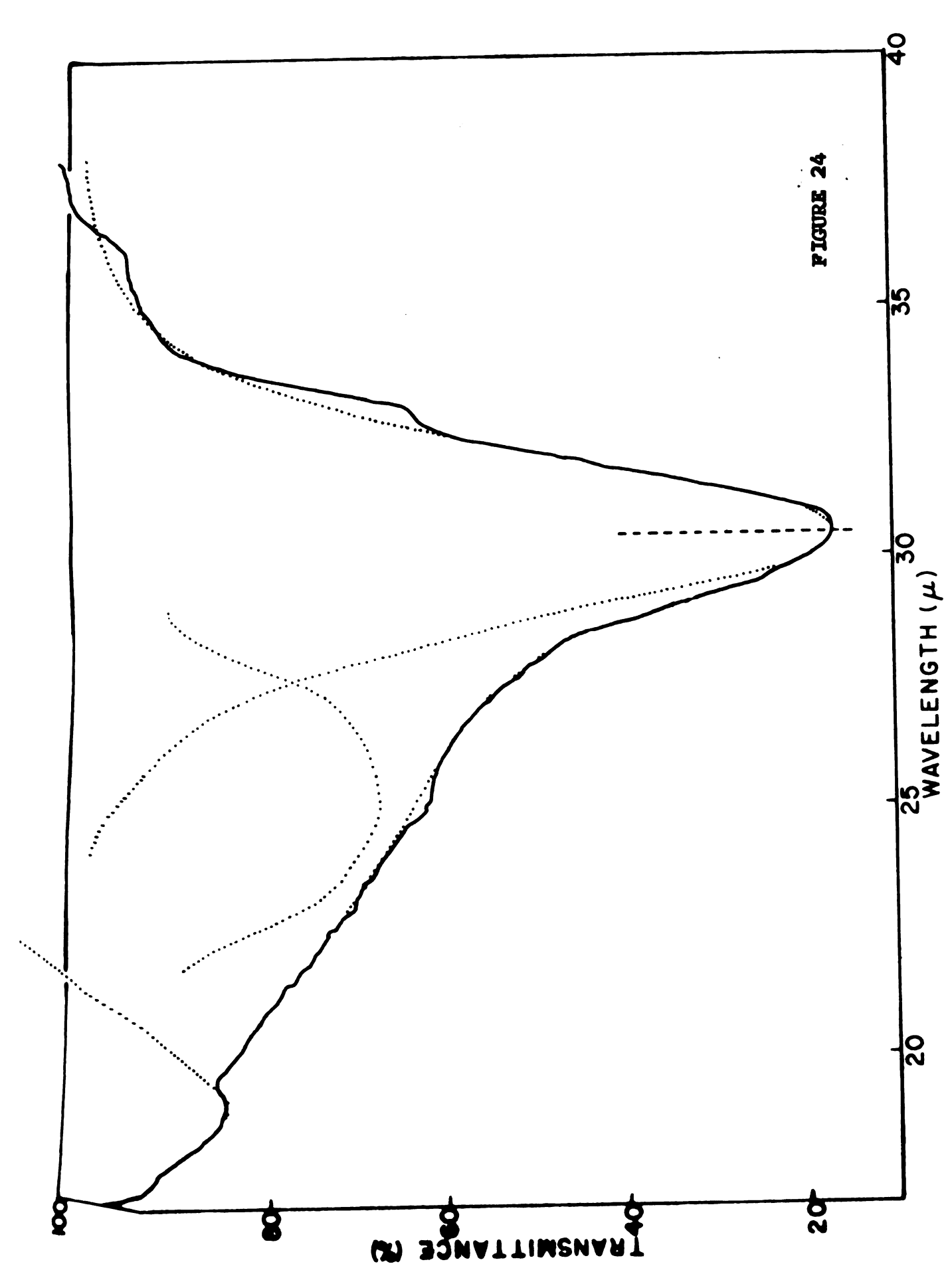


TABLE (2). γ/ω_0

%Li ⁶ F ¹⁹	% Li 7 F ¹⁹	γ/ω _ο
100	0	0.089
90	10	0.099
80	20	0.098
70	30	0.104
60	40	0. 106
50	50	0. 107
40	60	0.107
30	70	0.103
20	80	0. 106
10	90	0.096
0	100	0.099

B. Lithium Hydride

Part of the work on LiH was carried out with the Model 137 Perkin-Elmer spectrophotometer in the region 12.5 to 25 microns. The rest of the work was carried out with the Model 21 over the range 10 to 35 microns when it became available. The spectral region of interest for the study of LiH is nearly free of atmospheric interference. Unlike the work on LiF, where the isotopic mass of only the cation was varied, both the lithium isotopic mass and the hydrogen isotopic mass were varied. Figure 25 gives the average reduced mass of all the compositions of Li⁶ and Li⁷, H¹ and H². We notice that the greatest change in the reduced mass comes from replacing H¹ by H², of course. The change in the reduced mass is small when Li⁶ is replaced by Li⁷. In the work done with LiH, KBr windows were used most of the time, polyethylene windows being used only occasionally.

1. Effect of isotopic mass--Li⁶H¹, Li⁶H², Li⁷H¹, Li⁷H²:

The position of the dispersion wavelength of thin films of each of the four isotopically-pure compounds is listed below:

These films were evaporated in an atmosphere of hydrogen on KBr plates 1 inch in diameter and 1/8 inch thick. The thickness of these films is of the order of 0.01 to 0.1 microns. Replacing Li⁶ by Li⁷

REDUCED MASS OF LiH

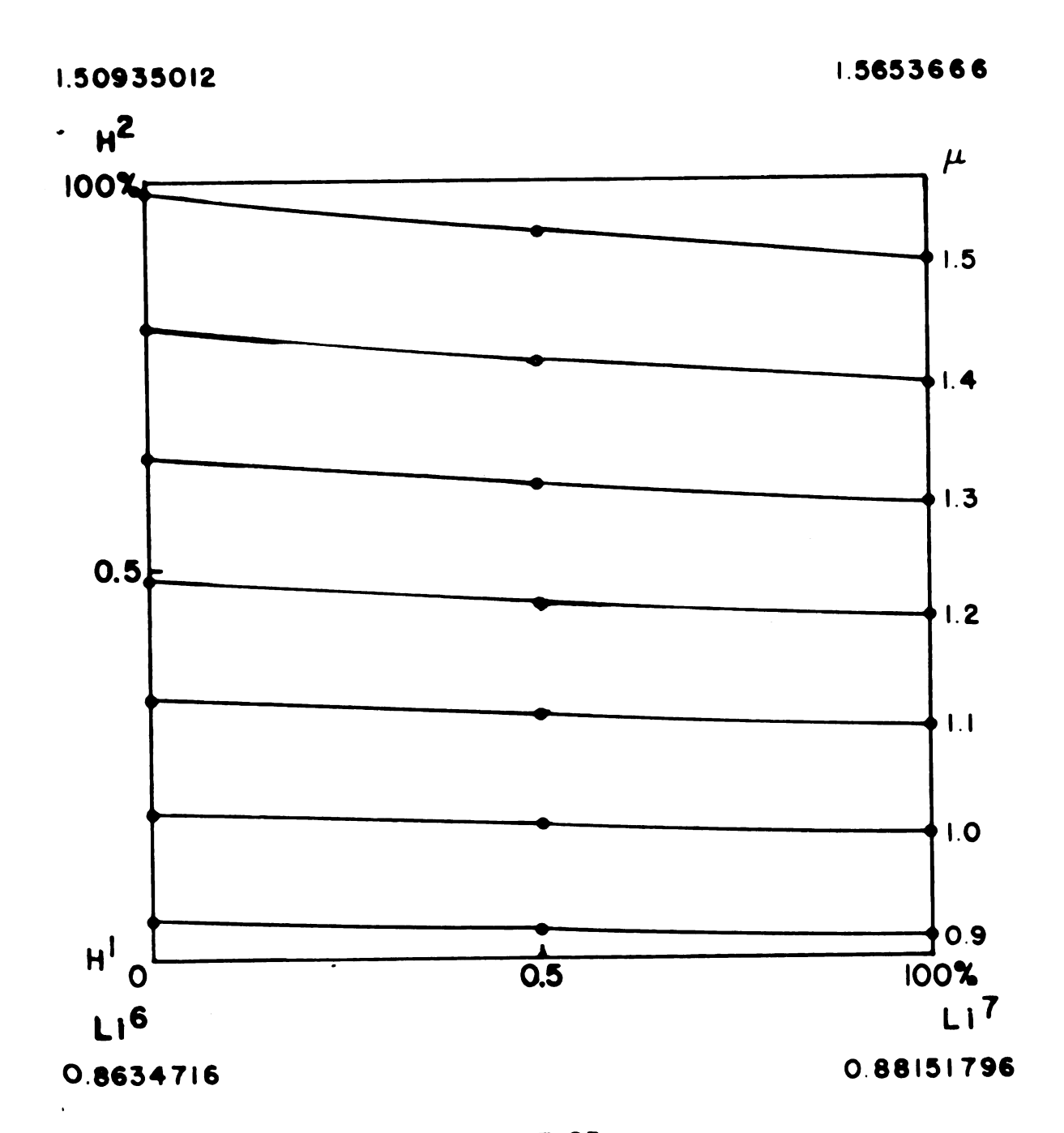


FIGURE 25

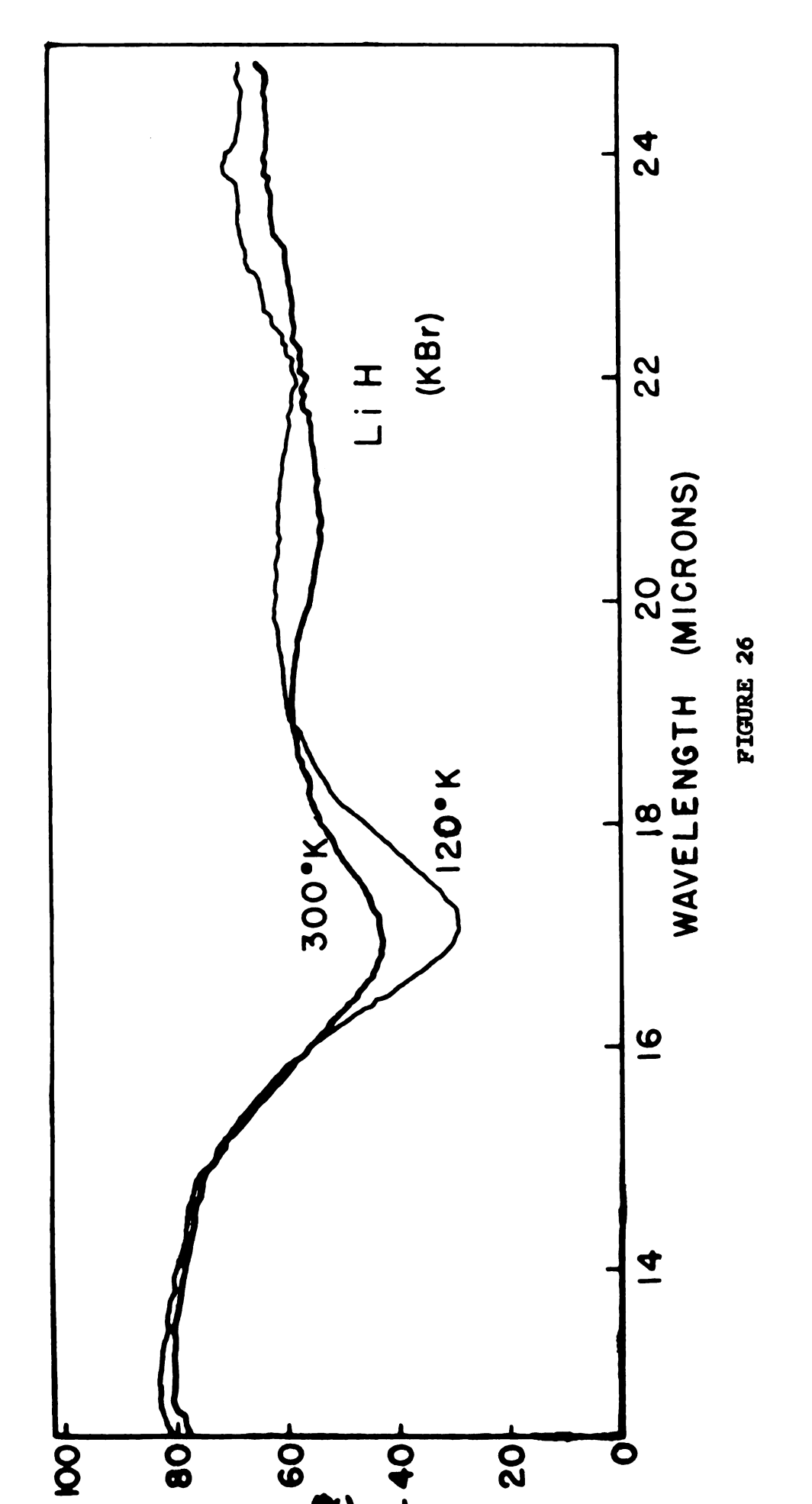
Lines of equal reduced mass for lithium hydride made of varying proportions of Li 6 , Li 7 , and H 1 , H 2 .

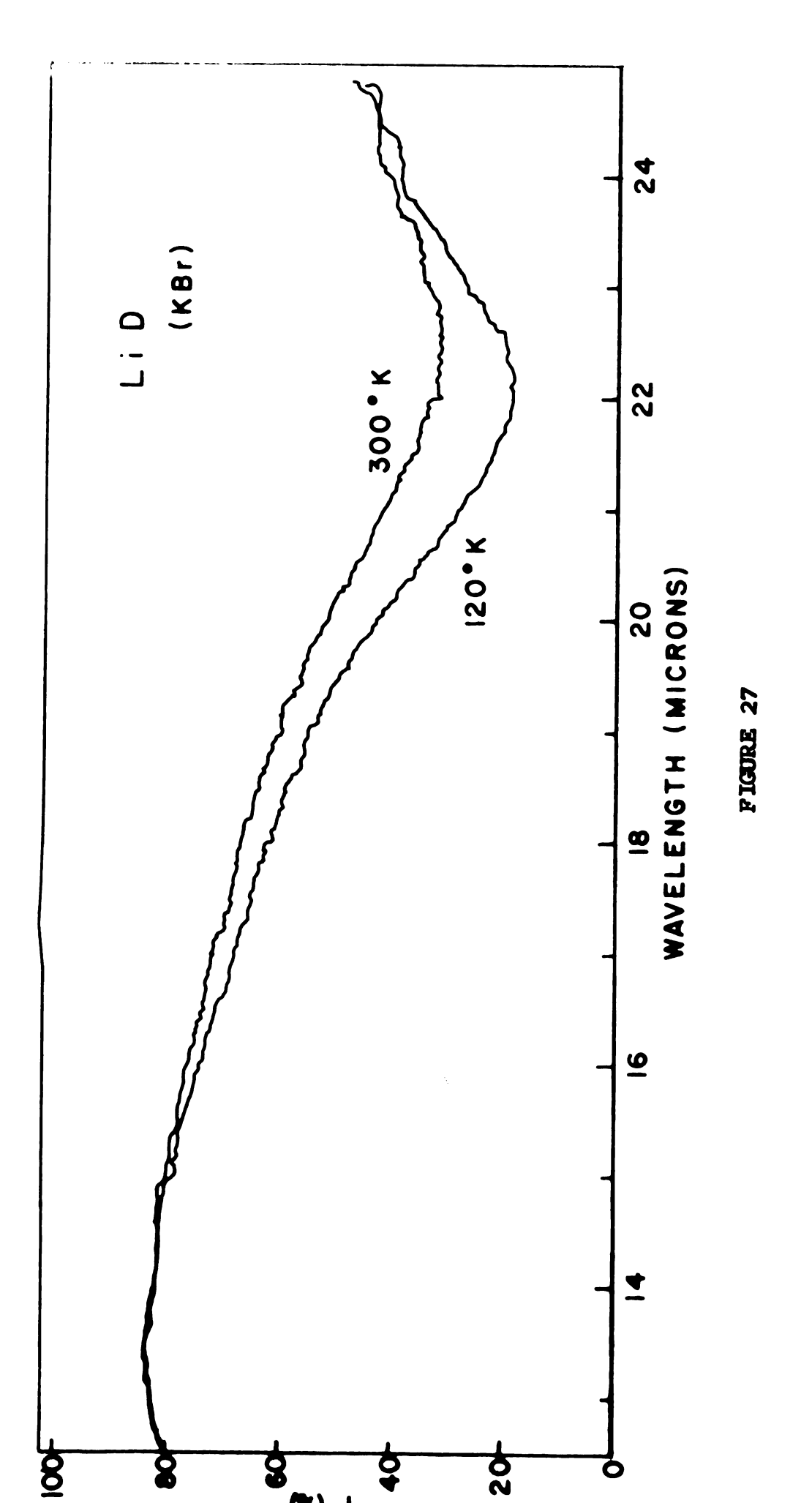
shifts the dispersion wavelength by a small amount, of the order of 0.2 micron, whereas replacing H¹ by H² shifts the dispersion wavelength by about 5.5 microns. These results are in agreement with those obtained by Zimmerman. Figures 26 and 27 show typical spectra as obtained with the spectrophotometer model 137. Spectra of LiH films show an auxiliary minimum around 20 microns. Figure 28 shows a spectrum of Li⁷H¹ film at 300°K superimposed on spectrum of Li⁷H² film when the abscissa has been multiplied by the reduced mass, again at 300°K. The close agreement between the theoretical prediction to be discussed later and the experimental results can be observed in this figure.

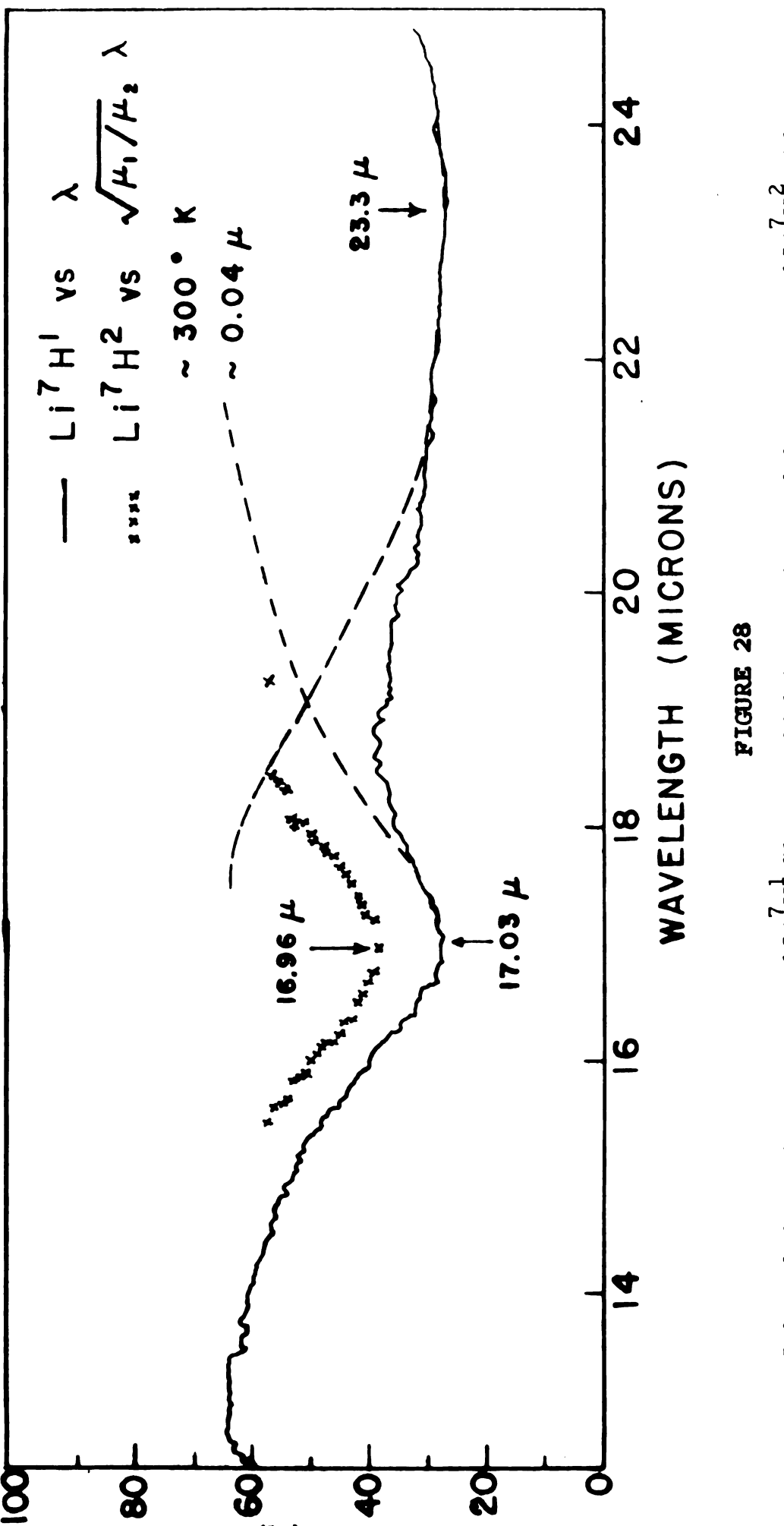
- 2. Effect of isotopic composition [xLi⁶H¹, (1-x) Li⁶H²], [xLi⁷H¹, (1-x) Li⁷H²]: Films of varying isotopic compositions of both Li⁶H¹, Li⁶H², and of Li⁷H¹, Li⁷H² were evaporated on KBr substrates and their spectra were studied. The results agree with those obtained by Zimmerman. Table 3 gives the reduced mass, and the wavelength of the absorption peaks from the various compositions used.
- 3. Effect of temperature: The spectra of thin films of Li⁶H¹, Li⁶H², Li⁷H¹, and Li⁷H² and their various mixtures were obtained at 120°K and at 300°K. At 120°K, the spectra of the Li⁶H² and Li⁷H² become deeper and narrower. The dispersion wavelength shifts toward shorter wavelengths by about 0.4 micron. The effect

Figure 26. Infrared absorption spectrum of Li⁷H¹ film evaporated onto KBr substrate. Temperatures: 300°K, 120°K.

Figure 27. Infrared absorption spectrum of Li⁷H² film evaporated onto KBr substrate. Temperatures: 300°K, 120°K.







Infrared absorption spectrum of Li 7 H film, on which is superimposed the spectrum of Li 7 H with abscissa multiplied by square root of reduced masses. Substrate: KBr; temperature, 300°K.

TABLE (3). Reduced masses and dispersion wavelengths

% Li ⁶ H ¹	%Li H	Average reduced mass	Dispersion wavelength	
100	0	0.864	16.97	
99	1	0.871	17.00	
98	2	0.876	17.00	
95	5	0.896	22. 20	
90	10	0.928	21, 13	
80	20	0.973	21. 15	
70	30	1. 057	21, 15	
60	40	1. 123	21.05	
50	50	1, 188	21.40	
40	60	1. 253	21.6	
30	70	1, 319	21, 17	
20	80	1. 386	21.9	
10	90	1. 449	22. 25	
0	100	1.550	22. 30	

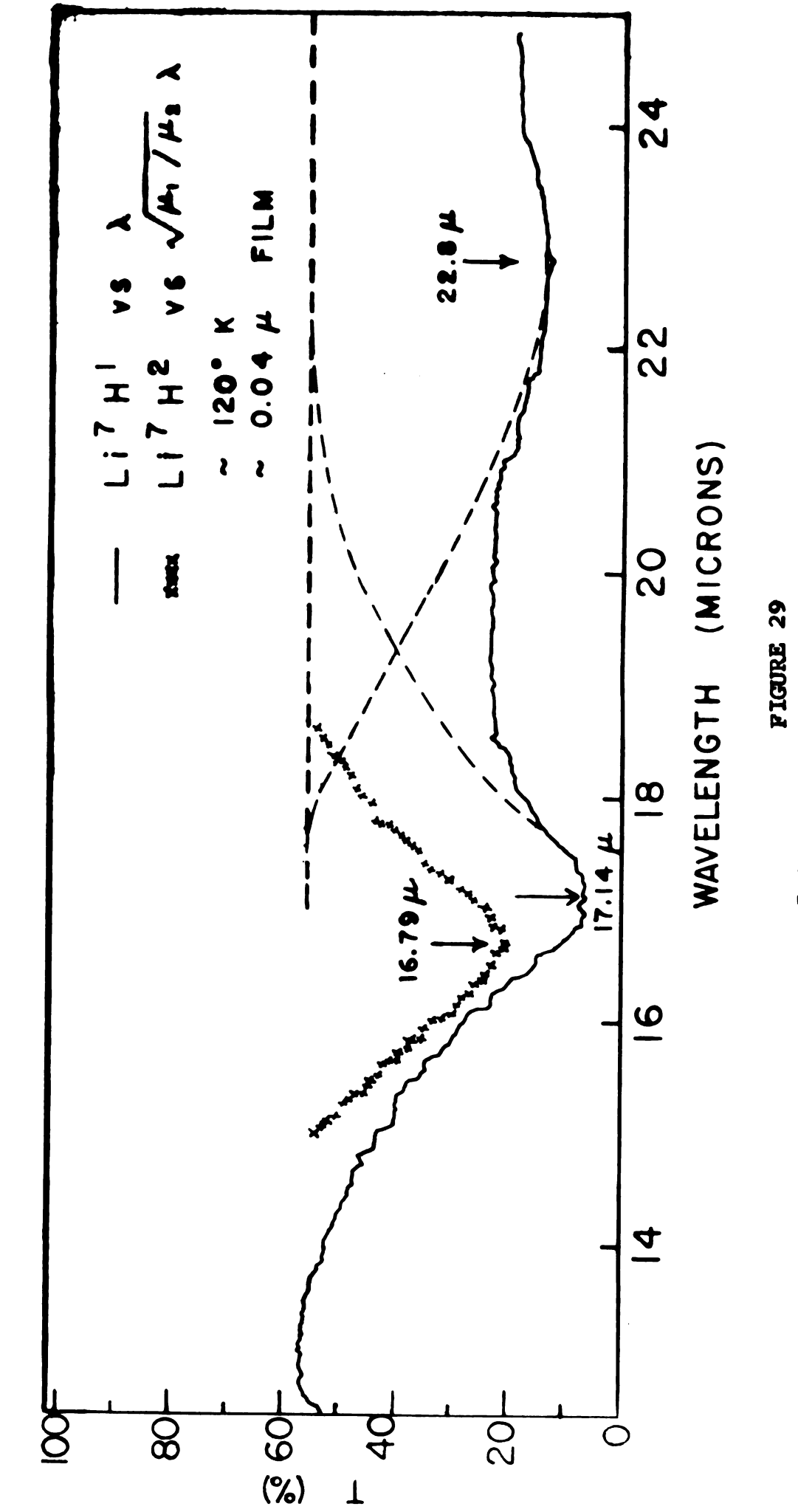
is seen in Figures 26 and 27. A similar effect is observed in the spectra of the isotopically-impure films. At 120°K, the spectra of the Li H and Li H films become narrower and deeper as expected, but the dispersion wavelength shifts by about 0.1 micron toward longer wavelengths. Figure 29 shows a spectrum of a Li H film at 120 K superimposed on a spectrum of Li H film for which the abscissa for the latter at 120 K has been multiplied by the square root of the ratio of the reduced masses. Contrary to theory--to be discussed later--the two peaks do not coincide. Some of the spectra of Li⁷H¹ film were taken at temperatures intermediate between 120°K and 300°K, and at temperatures higher than 300°K. Figure 30 shows the spectra of Li⁷H¹ at four different temperatures between 120°K and 300°K. These spectra were recorded as the liquid air in the chamber around the sample was evaporating, and the temperature of the sample was slowly rising. Figure 31 shows spectra of Li⁷H film at temperatures higher than 300°K. Higher temperatures were obtained using a chromel resistance wire wrapped around the sample holder as a heater.

4. Effect of substrate--potasium bromide, cesium bromide:

One-inch diameter and 1/8-inch thick plates of CsBr and KBr were

used as substrates for the evaporation of Li⁶H¹, Li⁶H², Li⁷H¹ and Li⁷H²

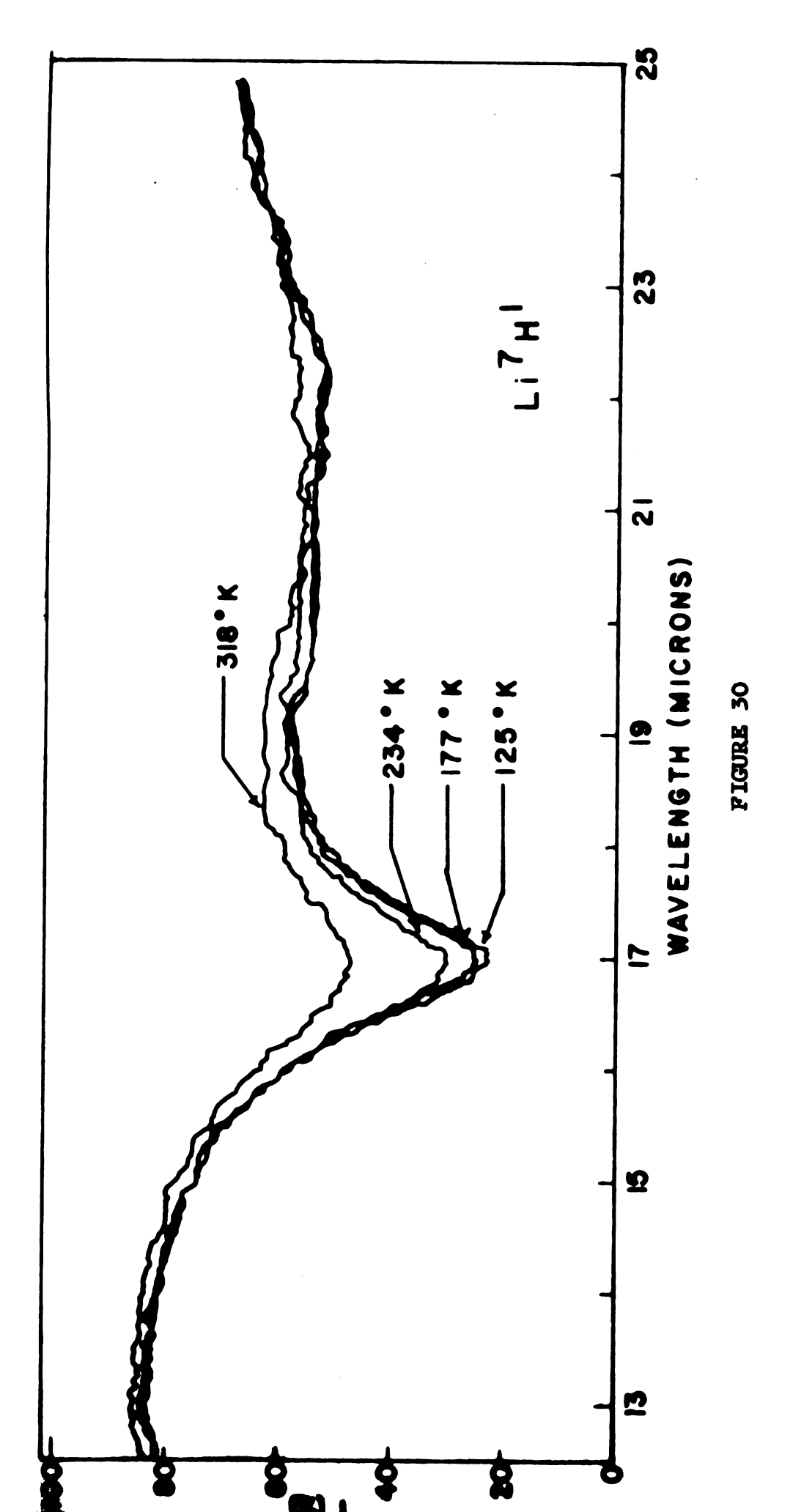
thin films; moreover, one-inch diameter and 0.04-inch thick polyethylene sheets were sometimes used. As was found for LiF, the

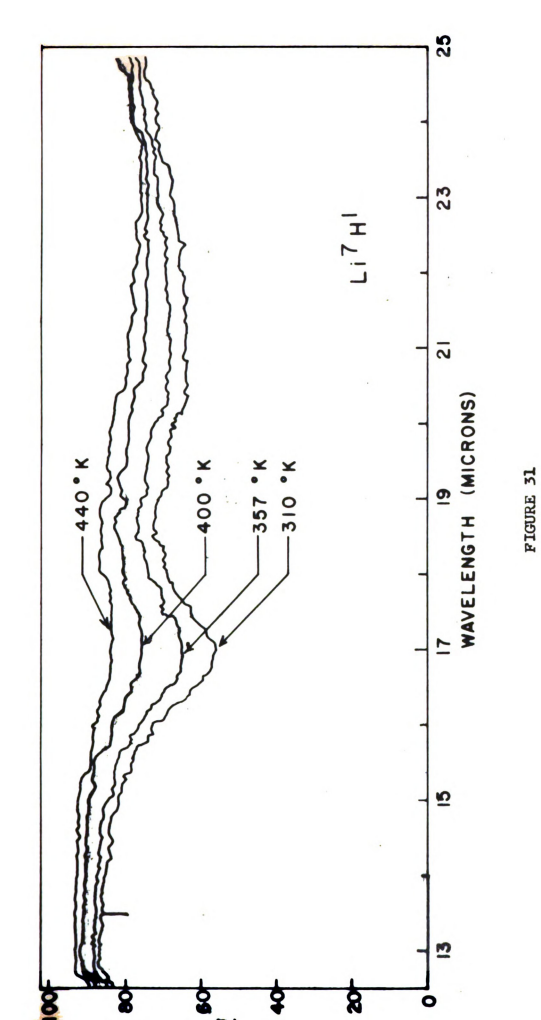


Infrared absorption spectrum of Li 7 H film on which is superimposed the spectrum of Li 7 H with abscissa multiplied by square root of reduced masses. Substrate: KBr; temperature, 120 K.

Figure 30. Infrared absorption spectrum of Li⁷H¹ evaporated onto KBr substrate. Temperatures: 125°K, 177° K, 234°K, and 318°K.

Figure 31. Infrared absorption spectra of Li⁷H¹ evaporated onto KBr substrate. Temperatures: 310°K, 357°K, 400°K, and 440°K.





position of the dispersion wavelengths of the thin LiH films seemed to depend to some extent on the substrate. Between 0.1 and 0.2 micron difference appears between the dispersion wavelengths of films evaporated on KBr and those evaporated on CsBr. Those evaporated on CsBr have the longer wavelength.

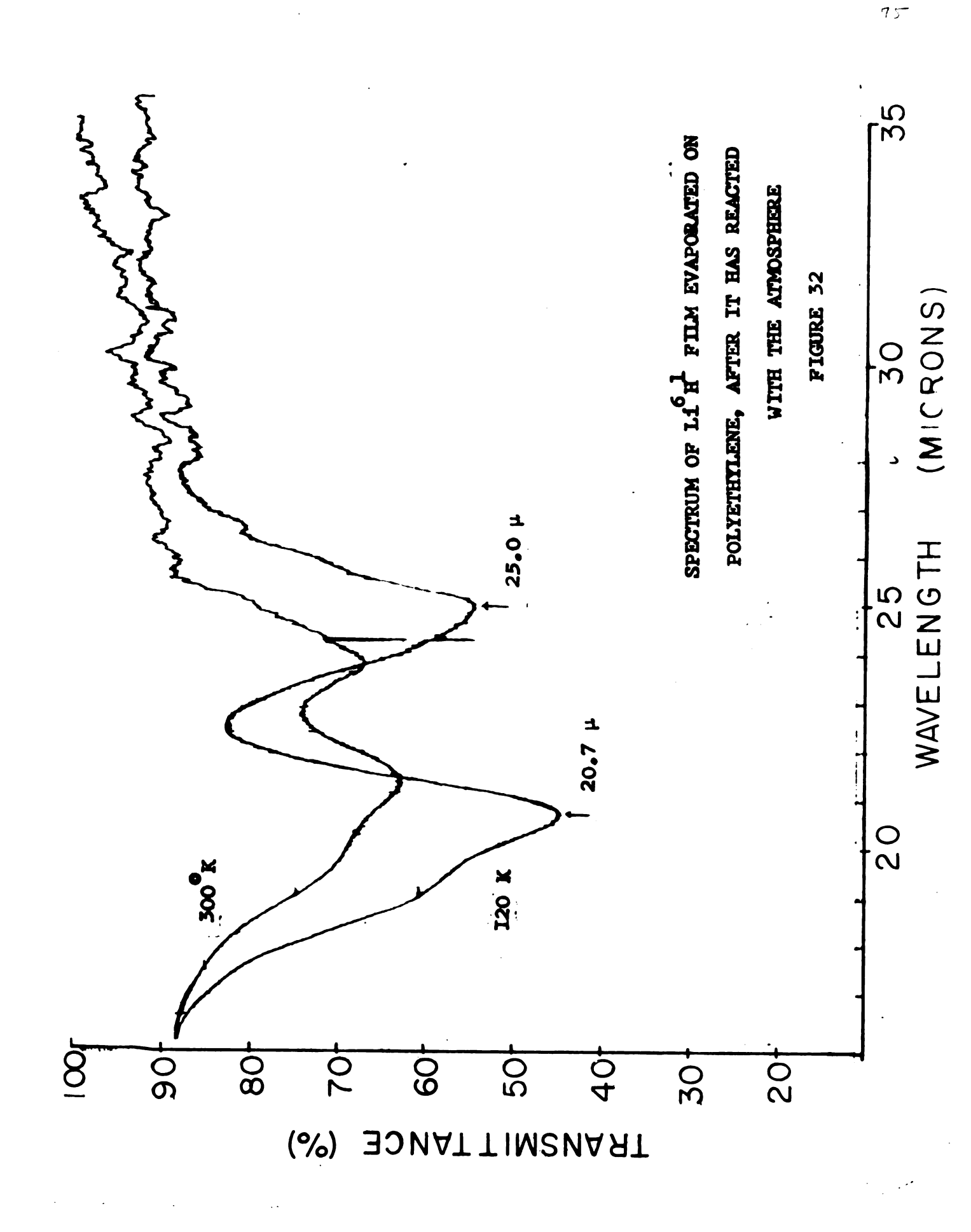
5. Effect of the atmosphere: As was mentioned in an earlier chapter, LiH reacts quickly with humid air. It was therefore necessary to store the LiH powder in a desiccator at all times. Films were evaporated in a vacuum, and kept in it during the entire experiment.

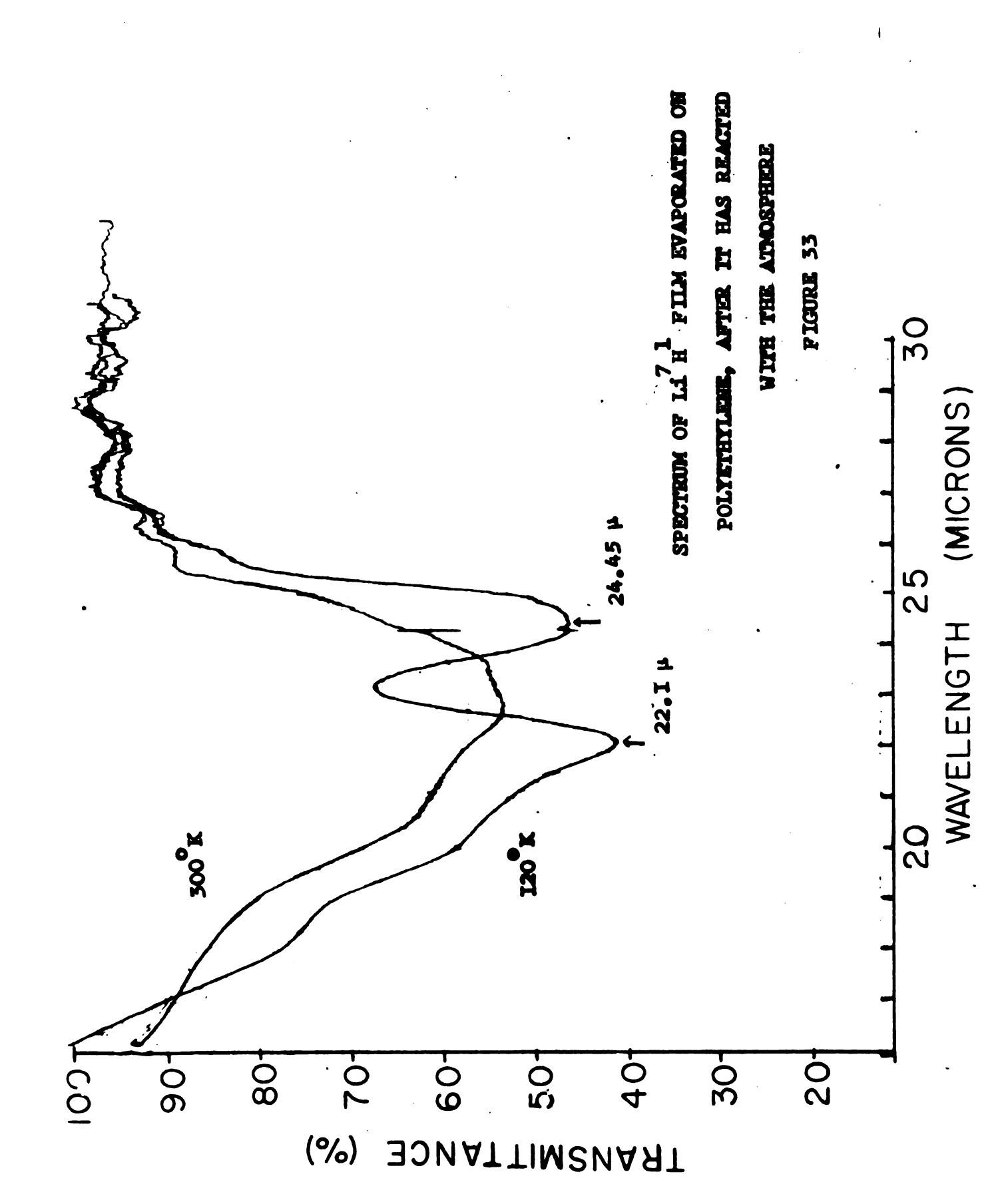
The shape of the spectrum begins to change as more and more LiH is changing to its oxide or hydroxide form. The rate of interaction depends of course on the vacuum and on the thickness of the film. When air is allowed to enter the cell, LiH changes completely to other forms, probably LiOH, H₂O. The spectra of the reacted films are completely different from the LiH spectra. Figure 32 shows the spectrum of a reacted Li⁶H¹ film at 300°K, and at 120°K. Figure 33 shows the spectrum of a reacted Li⁷H¹ film at 300°K and at 120°K. The spectra of reacted Li D have the same shape as those of reacted LiH spectra. Those of reacted composed films have the same shape as reacted LiH and LiD also.

6. Evaluation of λ_0 : Primarily we had arrived at the equation $\lambda_+ \lambda_- = \lambda_0^2$. This equation provides a means of calculating

Figure 32. Infrared absorption spectrum of Li⁶H¹ film evaporated onto polyethylene substrate, after reaction with atmosphere. Temperatures: 300°K, 120°K.

Figure 33. Infrared absorption spectrum of Li⁷H¹ film evaporated onto polyethylene substrate, after reaction with atmosphere. Temperature: 300°K, 120°K.



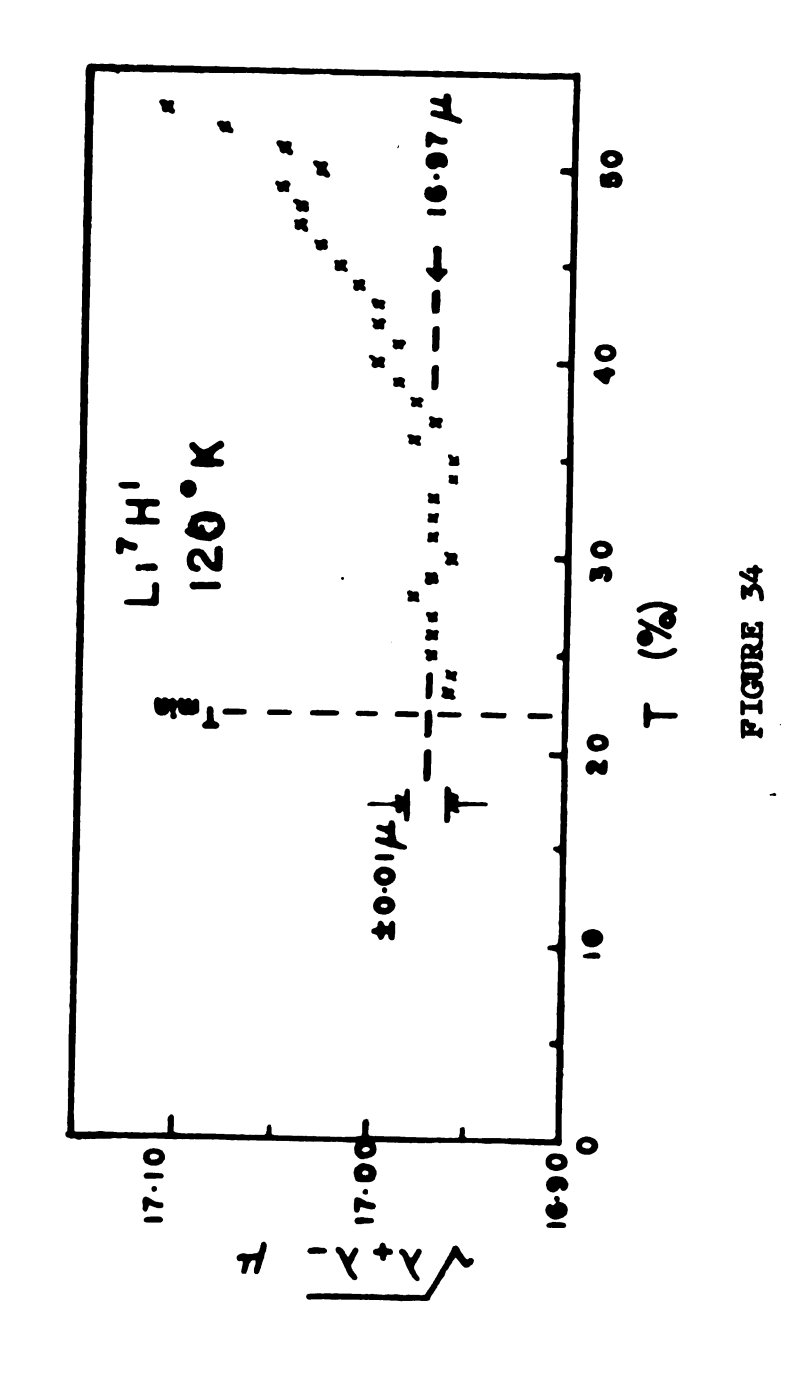


the dispersion wavelength accurately to within $\frac{1}{2}$ 0. 01 micron, since the spectra of the LiH and LiD films are uniform and are not affected much by atmospheric absorptions. Figure 34 demonstrates the precision of this method of measuring λ_0 ; from this figure we notice that $\lambda_-\lambda_+$ is fairly constant in the region around λ_0 . As an extension of procedure we may separate the peaks in the LiH and LiD spectra and in the reacted LiH and LiD films. Figure 35 demonstrates this technique as applied to a spectrum of Li 7 H 1 film at 2 CK.

7. Evaluation of γ/ω_0 : Equation (9) and equation (10) are used to calculate γ/ω_0 and γ/γ' for the films of LiH and LiD, shown in Figures 26 and 27. The results are listed below:

$$\frac{\gamma/\omega_{o}}{\omega_{o}}$$
 $\frac{\gamma/\gamma'}{\omega_{o}}$ LiH 0.1195 2.487 LiD 0.1877 2.060

 γ/γ' is the ratio of damping constant at 300°K to that at 120°K. Figure 36 shows a plot of $(\frac{\lambda_0}{\lambda} - \frac{\lambda}{\lambda_0})^2$ vs. $\frac{1}{T_0 - T_0} - \frac{1}{T_0 - T_{\min}}$ for aLi⁷H¹ film evaporated on KBr and recorded at 125°K. The curve is nearly a straight line indicating the accuracy of measuring γ/ω_0 .



Plot of $(\lambda_{+}\lambda_{-})^{1/2}$ as a function of transmission T for a spectrum of Li 7 H evaporated onto KBr substrate. Temperature: 120°K.

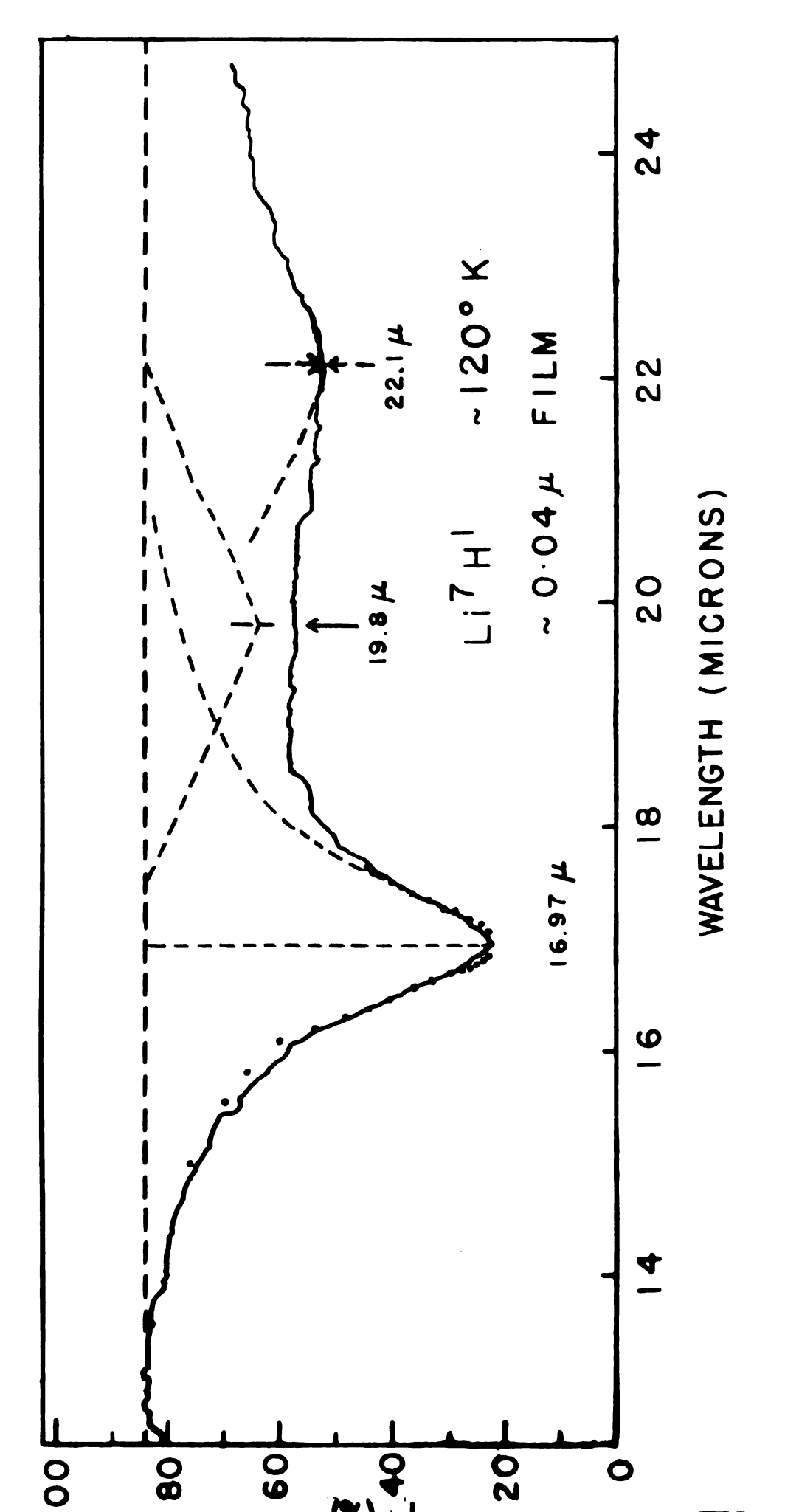


FIGURE 35

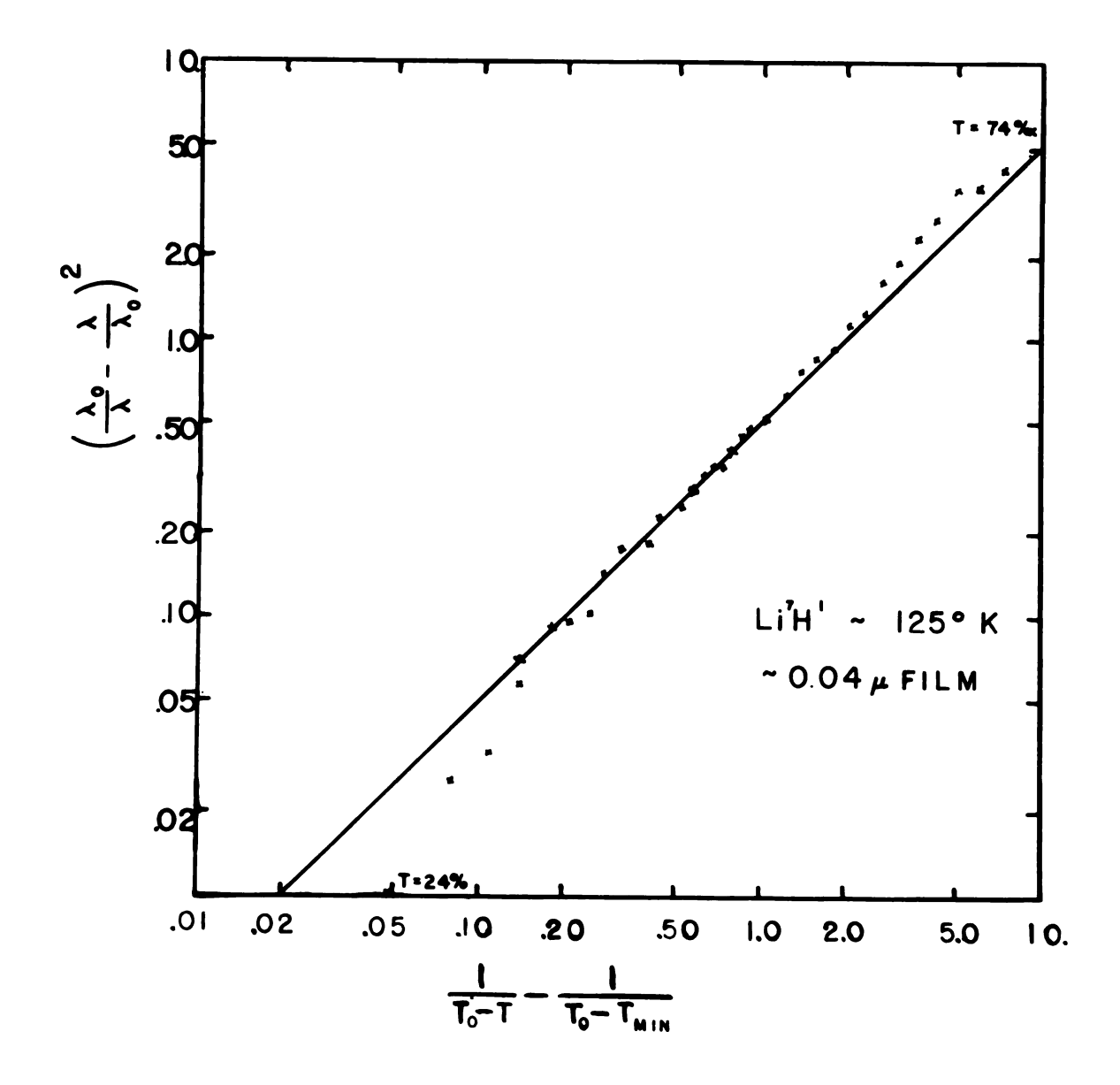


Figure 36. Plot of $\left(\frac{\lambda}{\lambda_0} - \frac{\lambda_0}{\lambda}\right)^2$ as a function of $\frac{1}{T_0 - T} - \frac{1}{T_0 - T_{\min}}$

for a spectrum of Li⁷H¹ evaporated onto KBr substrate. Temperature: 120°K.

V. DISCUSSION OF EXPERIMENTAL RESULTS

Comparison of present theory with experimental results requires knowledge of reflection data as well as transmission data; even then the theory contains parameters too difficult to be calculated. Hence we content ourselves with testing the predictions that follow from general arguments only.

A. Dispersion Wavelength $\lambda_0 = 2\pi c/\omega_0$

- 1. Effect of isotopic mass on λ_0 : Ordinarily the simple theory of lattice vibration is said to show that any characteristic frequency, for example, the infrared dispersion frequency, depends inversely on the square root of isotopic mass. Actually some general arguments, to be detailed shortly, show that this statement is not quite exact. It is however a very good approximation, and we shall accordingly test it directly. In Table 4 are summarized the infrared dispersion wavelengths and the reduced masses for all the isotopically pure substances at all the temperatures and substrates that we have used; in addition are listed the ratios of the dispersion wavelengths to the ratio of the reduced masses, in each case the heaviest substance being used as a reference.
- 2. Effect of isotopic composition on λ_0 : Although it is not clear what effect isotopic composition has on the position of the dispersion wavelength, it is natural to try to correlate the position with

TABLE (4). Effect of isotopic mass on infrared dispersion wavelength

	μ/μ _s	Polyet $\frac{300^{\circ} K}{\lambda/\lambda_{s}}$	hylene $\frac{120^{\circ} K}{\lambda/\lambda_{s}}$	$\frac{300^{\circ} K}{\lambda/\lambda_{s}}$		$\frac{300^{\circ} K}{\lambda/\lambda_{s}}$	$\frac{120^{\circ} K}{\lambda/\lambda_{s}}$
Li ⁶ F ¹⁹	0.941	0.947		0.948 1.000		-	-
Li ⁶ H ¹ Li ⁶ H ² Li ⁷ H ¹ Li ⁷ H ²	0.746 0.987 0.754 1.000	- - -	- - -	0.758 0.996 0.760 1.000	0.773	0. 756 0. 993 0. 759 1. 000	0. 769 0. 993 0. 774 1. 000

the average reduced mass of the substance under study. Even then, it is not clear whether the arithmetic mean is superior to the harmonic mean. The difference between these two means, however, is slight, and hence we test only the arithmetic mean. Table 5 lists the compositions of LiF¹⁹ used, evaporated onto CsBr and polyethylene substrates and recorded at 300°K, and 120°K. Here the ratios

$$w_{x} = \frac{\lambda_{ox}/\lambda_{oo}}{(\mu_{x}/\mu_{s})^{1/2}}$$

which should equal unity according to the simple assumption just mentioned, is given for the varying compositions of LiF¹⁹. The departure from unity is slight, amounting on the average to only a few parts per thousand. The values for CsBr substrate are a little more regular than those for polyethylene.

For LiH, the shift of λ_{0} with isotopic composition is so irregular it is not worth-while to tabulate the results here.

3. Effect of temperature on λ_0 : Lithium fluoride: A cross plot prepared from Figures 22 and 23 is shown in Figure 37, a plot of dispersion wavelength against temperature for selected compositions of LiF¹⁹. The average shift (1. $25\mu/180 \text{ K-deg}$)/31. $5\mu \sim 2 \times 10^{-4}/\text{K-deg}$. In the absence of strong interaction with the substrate, this coefficient should roughly equal that of the temperature coefficient of the elastic modulus of LiF, namely, 3. $5 \times 15^{-4}/\text{K-deg}$. The argument is probably satisfactory.

TABLE (5). Effect of isotopic composition on dispersion wavelength for $\text{Li}^{6\frac{\pi}{F}19}$

	CsBr substrate				P. E substrate			
	30	0°K	120 ⁰ K		300°K		120 [°] K	
x	λ _{ox}	ω ×	λ ox	ω x	λ _{ox}	ω ×	λ _{ox}	ω x
0. 0	31.0μ	1.004	29.9μ	1. 005	30. 8μ	1.004	29. 5μ	1.008
0.1	30. 9	0.994	29.8	0.995	30. 9	1.000	29. 3	0.994
0.2	31.3	1.001	30.1	0. 999	31.2	1.004	29. 3	0.985
0.3	31.5	1.000	30. 4	1.002	31.3	1.000	30. 1	1.008
0.4	31.7	1.001	30. 5	0. 999	31.4	0.997	30.2	1.006
0. 5	31.8	0.998	30.7	1.000	31.5	0.995	30.5	1.010
0.6	32. 0	0.998	30.7	0.994	31.6	0.992	30.6	1.009
0.7	32. 2	1.000	30.9	0.995	31.7	0.990	30.5	0.999
0.8	32. 3	0.997	31.0	0.994	31.4	0.992	30.8	1.003
0.9	32. 4	0.995	31.3	0. 998	32. 1	0.993	30. 9	1.001
1.0	32. 7	1.000	31.5	1.000	32. 5	1.000	31.0	1.000

Lithium hydride: Figure 38 shows the variation of λ_0 with temperature for LiH and LiD. The behavior for LiH is indeed anomalous, and we are hesitant to consider the increase in λ_0 real without additional study.

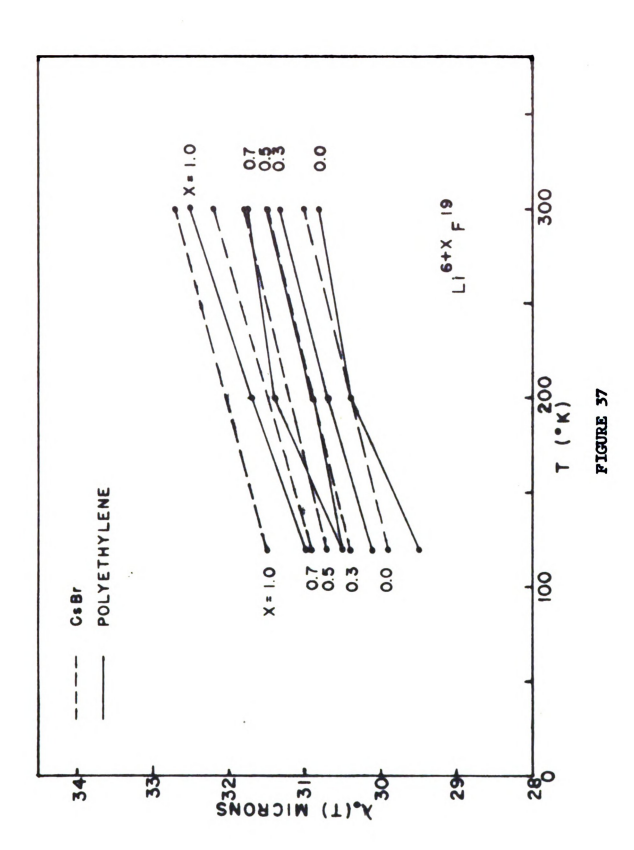
4. Effect of substrate on λ_0 : From Table 5 one observes that the dispersion wavelength for LiF on polyethylene is a few tenths of a micron smaller than that on CsBr. Since there is negligible absorption by either substrate in this region of the spectrum, and since the elastic modulus for LiF is much higher than that of either polyethylene or CsBr, we are at a loss to give a plausible explanation for this shift. Although epitaxy is more likely to be encountered with Cs Br substance, we cannot at this stage ascribe the shift to this effect.

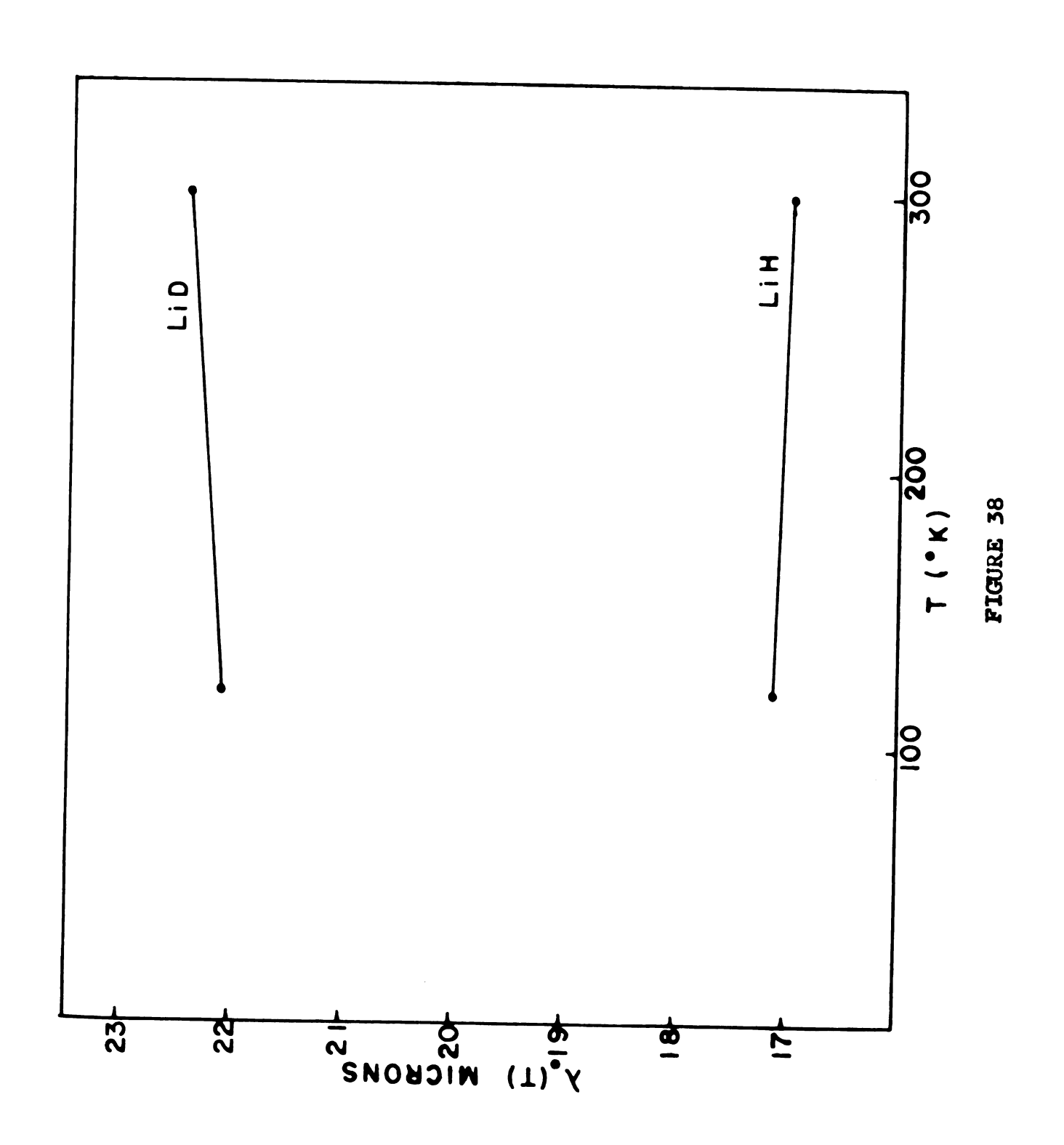
B. Damping Constant γ/ω_0

- 1. Theoretical considerations: The general arguments that we wish to make are the following:
 - a. The equation of motion for isotopically-pure substances in the Newtonian formulation contains mass and time on one side only of the equation of motion, in the form of mass times a second order time derivative of spatial coordinates. The other side of the equation contains only spatial coordinates and atomic parameters other than mass.

Figure 37. Dependence of infrared dispersion wavelength on absolute temperature for LiF¹⁹ films of various isotopic compositions evaporated onto CsBr and onto polyethylene.

Figure 38. Dependence of infrared dispersion wavelength on absolute temperature for LiH and LiD films evaporated onto KBr.





Therefore the solutions can contain time and mass only in the combination: time/square root of mass, and hence all frequencies must be related by the condition $\omega_0 M^{1/2} = \text{constant}; \text{ or if equivalent temperatures are introduced in place of frequencies through the relation}$ $-h\omega = k\theta, \text{ then } \theta M^{1/2} = \text{constant}. \text{ Specifically we may}$ conclude that the lattice-vibrational frequency distribution can differ between isotopes only by a scale factor equal to the ratio of the square root of the masses.

- b. General dimensional considerations show that the temperature must enter only in the ratio of KT, the average thermal energy, to $\hbar\omega_c$, where $\omega_c = k \frac{\theta}{c}/\hbar$ in some characteristic frequency inversely proportional to $M^{1/2}$.
- c. Therefore comparisons between various phenomena dependent on lattice-vibration interactions should be made at equal reduced temperature T/θ .
- d. In the case of isotopically-impure substances, part "a" of the above argument breaks down; nevertheless calculations on the change of lattice-vibrational spectrum by introduction of lattice impurities, suggest that the effect of isotopic substitution can be taken into account by averaging the isotopic mass in some way. This view cannot be completely correct, although for many phenomena,

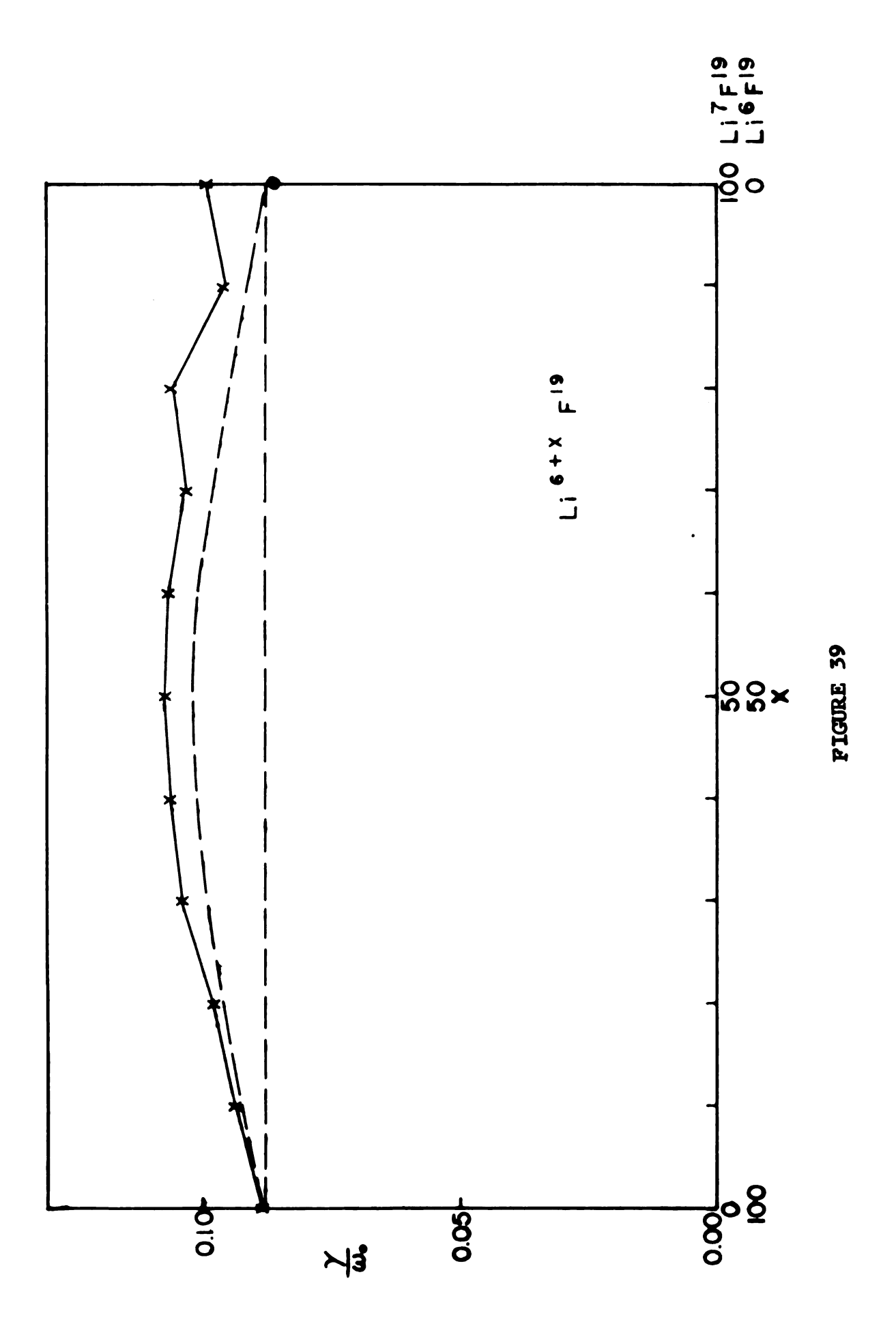
it would appear to have validity. Thus we have seen that for a position of absorption maximum, i.e., the dispersion wavelength, the shift with isotopic composition was accounted for by use of an average isotopic mass; but now we shall see that for the width of absorption band, which is proportional to γ/ω_0 , the solution is not quite so simple.

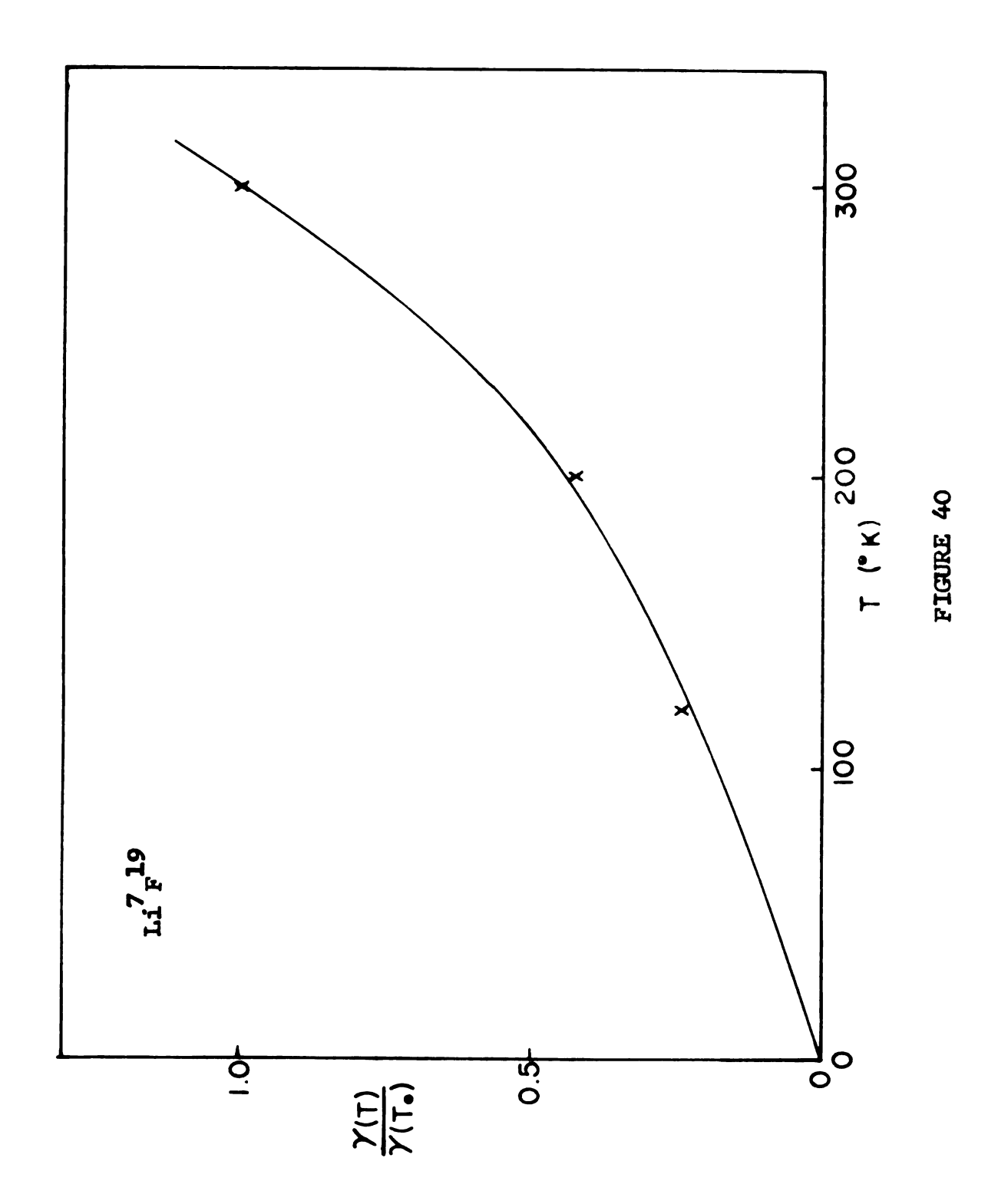
2. Consideration of experimental results: To illustrate these ideas, we look at the solid curve in Figure 39, a plot of γ/ω_0 against isotopic composition for ${\rm LiF}^{19}$ evaporated on polyethylene and observed at $300^{\circ}{\rm K}$. One notices that the absorption coefficient increases as the proportion of ${\rm Li}^7$ is increased, falling slightly as isotopically pure ${\rm Li}^7{\rm F}^{19}$ is reached. The last value is somewhat higher than that for isotopically pure ${\rm Li}^6{\rm F}^{19}$, but according to paragraph "c" above, comparison should not be made at the same absolute temperature, but at the same reduced temperature.

Theory does not give adequate guides as to the dependence of γ/ω_0 on the absolute temperature T, hence we make use of our experimental data as shown in Figure 40. The absolute temperature for ${\rm Li}^7 {\rm F}^{19}$ corresponding to the reduced temperature for ${\rm Li}^6 {\rm F}^{19}$ at room temperature is $300^{\circ}/1.059 = 282^{\circ}{\rm K}$. From the graph we can estimate then the value for damping constant for ${\rm Li}^7 {\rm F}^{19}$ to be 0.086, in comparison with 0.088 for ${\rm Li}^6 {\rm F}^{19}$. The values do not agree perfectly, but

Figure 39. Plot of γ/ω_0 against isotopic compositions for LiF 19 evaporated onto polyethylene and recorded at $300^{\rm O}K.$

Figure 40. Variation of γ with absolute temperature for Li $^7F^{19}$ film evaporated onto polyethylene substrate.





they are close enough to indicate the power of this argument. For isotopically impure lithium fluoride, we note that this procedure does not reduce γ/ω_0 to a constant value, but rather that there seems to be an increase due to the mixing. Hence it is clear from the solid line that mere scaling alone will not bring absorption spectra for isotopically-impure substances into coincidence; and from the dashed curve, it is clear that although use of a scaling factor in conjunction with comparison at equal reduced temperature suffices to account for isotopic-mass effect in isotopically pure compounds, it does not account for it in isotopically-impure compounds.

The effect of substrate is slight and we have not yet been able to deduce much information from it.

LiH has proved to be less tractable than LiF. This circumstance is undoubtedly due both to imperfections in experimental technique and to the rather complicated chemical bonding in this substance. The potential value of investigations with lithium hydrite, if improved methods of experiment and analysis can be developed, is high.

REFERENCES CITED

- 1. M. Lax and E. Burstein, Phys. Rev. 97, 39 (1955).
- 2. R. B. Barnes, R. R. Brattain, and F. Seitz, Phys. Rev. 48, 582 (1935).
- 3. B. Szigeti, Proc. Roy. Soc. A255, 217 (1956).
- 4. R. F. Wallis and A. A. Maradudin, private communication.
- 5. R. B. Barnes, Zeit. f. Phys. 75, 723 (1932).
- 6. R. W. H. Stevenson and Nattley, Nature, 182, 471 (1958).
- 7. G. von Heilman, Zeit. Naturf. 13a, 238 (1958).
- 8. H. W. Hohls, Ann. Phys., 29, 433 (1937).
- 9. M. Klier, Zeit. f. Phys., 150, 49 (1958).
- 10. C. Haas and J. A. A. Ketelaar, Phys. Rev. 103, 564 (1956).
- 11. M. Gottlieb, Ph. D. thesis, University of Pennsylvania (1959).
- 12. D. J. Montgomery and R. H. Misho, Nature, 183, 103 (1959).
- 13. W. W. Watson, Phys. Rev., 25, 887 (1925).
- 14. G. Nakamura, Zeit. f. Phys. Chem. Abt. B, 3, 80 (1929).
- 15. F. H. Crawford and T. Jorgensen, Phys. Rev., 46, 749 (1934).
- 16. W. Klemperer, J. Chem. Phys., 23, 2452 (1955).
- 17. R. Velasco, Can. J. Phys., 35, 1204 (1957).
- 18. A. S. Filler and E. Burstein, Bull. Amer. Phys. Soc., <u>5</u>, 198 (1960).
- 19. B. Zimmerman, Ph. D. thesis, Michigan State University (1960).
- 20. M. Born and K. Huang, <u>Dynamical Theory of Crystal Lattice</u> (Oxford at Clarendon Press, 1954), Chapt. 2.

Man Circi PHYSICS-MATH LIB.

MICHIGAN STATE UNIV. LIBRARIES